ERDC/GSL TR-15-26

Geotechnical and Structures Laboratory

US Army Corps
of Engineers®
Engineer Research and
Development Center

ERDC
INNOVATIVE SOLUTIONS
for a safer, better world

Unconventional Hydrocarbon Development Hazards Within The Central United States

Report 1: Overview and Potential Risk to Infrastructure

Oliver-Denzil S. Taylor, Alanna P. Lester,
and Theodore A. Lee III

August 2015

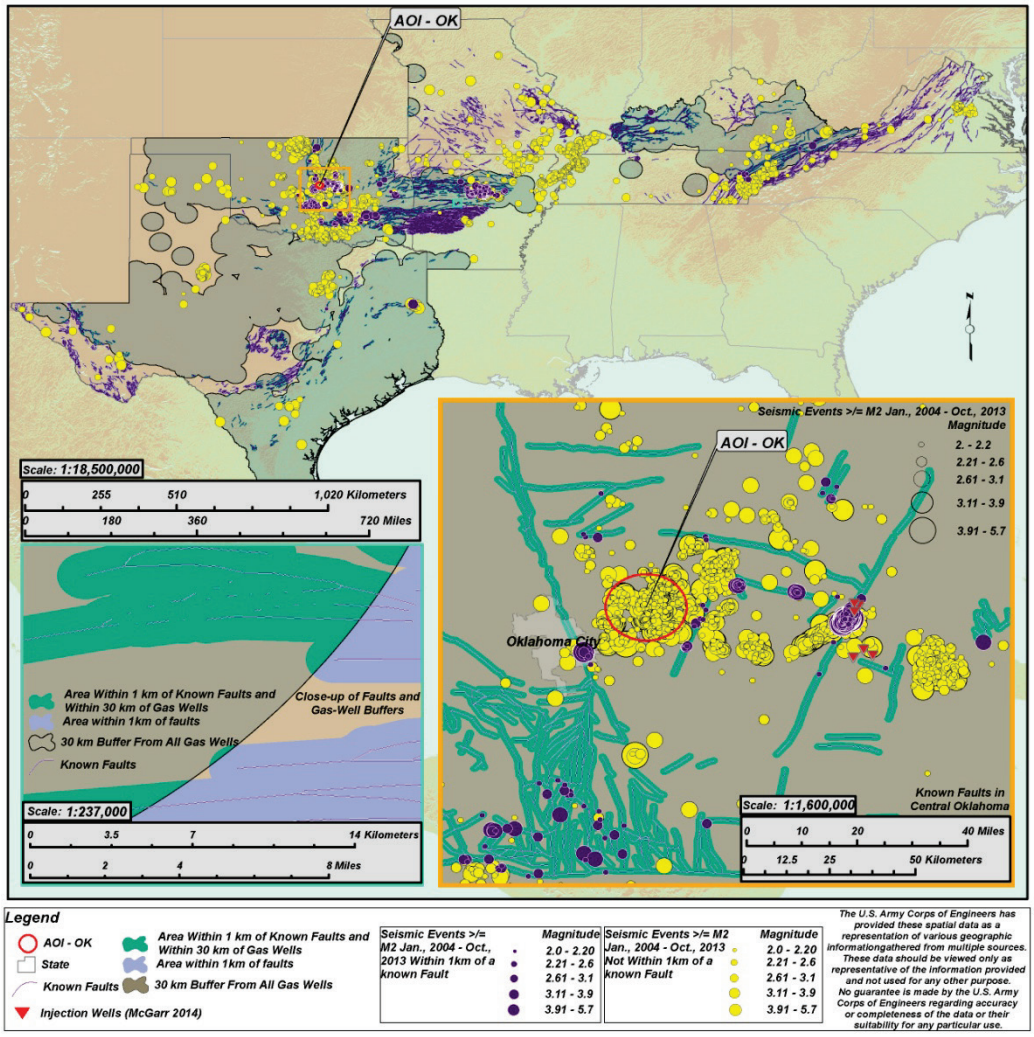

Approved for public release; distribution is unlimited.

The U.S. Army Engineer Research and Development Center (ERDC) solves the nation's toughest engineering and environmental challenges. ERDC develops innovative solutions in civil and military engineering, geospatial sciences, water resources, and environmental sciences for the Army, the Department of Defense, civilian agencies, and our nation's public good. Find out more at www.erdc.usace.army.mil.

To search for other technical reports published by ERDC, visit the ERDC online library at http://acwc.sdp.sirsi.net/client/default.

ERDC/GSL TR-15-26
August 2015

Unconventional Hydrocarbon Development Hazards Within The Central United States

Report 1: Overview and Potential Risk to Infrastructure

Oliver-Denzil S. Taylor, Alanna P. Lester, and Theodore A. Lee III

Geotechnical and Structures Laboratory
U.S. Army Engineer Research and Development Center
3909 Halls Ferry Road
Vicksburg, MS 39180-6199

Report 1 of a series

Approved for public release; distribution is unlimited.

Prepared for U.S. Army Corps of Engineers
Washington, DC 20314-1000

Abstract

Unconventional hydrocarbon development-induced seismic hazard in historically aseismic regions is more frequent and concentrated than seismicity in established tectonic high-hazard zones. A significant increase in seismicity within historically aseismic regions and in close proximity to federal infrastructure has been observed within Arkansas, Kentucky, Missouri, Oklahoma, Tennessee, Texas, and Virginia. Seismological events **M**2.0 and greater, spanning 02/08/1950 until 10/20/2013, were analyzed to identify and assess the hazard potential. Geospatial and temporal observations correlate the seismic increase to the rise of unconventional hydrocarbon development, which has become more analogous with deep ore mining in terms of energy release. Thus, unconventional hydrocarbon is subjected to the same causality phenomena and associative hazards with significant implications towards quantifying the risk to infrastructure health and longevity. Furthermore, the current standard of practice for risk assessment is not applicable for this highly variable, induced hazard. Additionally, this research investigated the cumulative seismic potential, based on injected fluid volume, of co-located hydraulic fracturing wells wherein the seismic potential of such wells are equivalent to the seismic potential of conventional wastewater injection wells. This cumulative seismic potential of multiple hydraulic fracturing wells could explain the seismicity within regions of Arkansas, Oklahoma, and Texas, wherein no other regional geo-engineering activity has been reported. Additionally, this study presents a power-law relation, useful for all injected fluid activities irrespective of the injection purpose, and applies the cumulative potential to the largest known UHP hydraulic fracturing volumes an event up to M_w5.5 can reasonably expect with a maximum potential of M_w6.5.

DISCLAIMER: The contents of this report are not to be used for advertising, publication, or promotional purposes. Citation of trade names does not constitute an official endorsement or approval of the use of such commercial products. All product names and trademarks cited are the property of their respective owners. The findings of this report are not to be construed as an official Department of the Army position unless so designated by other authorized documents.

DESTROY THIS REPORT WHEN NO LONGER NEEDED. DO NOT RETURN IT TO THE ORIGINATOR.

Contents

Figures and Tables

Figures

Tables

Preface

This study was conducted for the U.S. Army Corps of Engineers under the U.S. Army Engineer Research and Development Center as a component of the Remote Assessment of Critical Infrastructure work package.

The work was performed by the Structural Engineering Branch (GS-S) of the Geosciences and Structures Division (GSD), and USACE Reachback Operations Center (GU) U.S. Army Engineer Research and Development Center, Geotechnical and Structures Laboratory (ERDC-GSL). At the time of publication, Charles W. Ertle was Chief, CEERD-GS-S; and Bartley P. Durst was Chief, CEERD-GSD. Rhonda Taylor was the Director, CEERD-GU. The Acting Deputy Director of ERDC-GSL was Dr. Gordon W. McMahon, and the Acting Director was Dr. William P. Grogan.

LTC John T. Tucker III was the Acting Commander of ERDC, and Dr. Jeffery P. Holland was the Director.

Unit Conversion Factors

All units are in metric.

Multiply	By	To Obtain
Dyne-centimeter	10^7	newton meters
feet	0.3048	meters
miles	1.6093	kilometers
pounds (force) per square inch	175.1268	kilopascals

1 Introduction

Infrastructure in regions of historically significant seismicity is designed to meet certain seismic hazards criteria; thus, there must be realistic understanding of source potential in the context of past seismicity and current seismic trends for those locations. The current standard of practice to determine the associative risk is through the means of a Probabilistic Seismic Hazard Analysis, PSHA, using a model of a memory-less stationary homogeneous Poisson process with a constant, time-independent frequency of occurrence (McGuire 1995):

$$\gamma(a) = \sum_{i=1}^{S} \nu_i \iiint f_{M,i}(m) f_{R,i}(r \mid m) f_{\varepsilon,i}(\varepsilon) P[A > a \mid m, r, \varepsilon] dr dm d\varepsilon \quad (1)$$

where $\gamma(a)$ is the annual probability of exceedance of a ground motion amplitude, a; $f_{M,i}(m)$ is the probability density function of magnitude; $f_{R,i}(r|m)$ is the probability density function for the site-to-source distance; $f_{\varepsilon,i}(\varepsilon)$ is the ground motion probability density function; ε is the ground motion uncertainty; $P[A > a]$ is the probability that the ground motion, A, will exceed a threshold value, a, for a given m, r, and ε; S is the number of seismic sources affecting the structure of interest; and ν is the frequency of occurrence for a seismic source. However, this analysis assumes that future events can be extrapolated from past seismic observations. This fundamental assumption predicates that the regional seismic rate is constant, that the statistical distribution is representative of any time period, and that the source locations are well constrained. The requirement to properly assess both *hazard* and *risk* to federal infrastructure in these regions of increased atypical seismic activity without historical precedent became the driving force for the research presented herein.

The Geotechnical and Structures Laboratory (GSL) of the U.S. Army Engineer Research and Development Center (ERDC) has a mission to support research on maintaining water-resource infrastructure. Recent research by ERDC focused on providing engineers, embankment owners, and regulatory agencies with a multi-hazard analysis tool to identify critical hazard conditions that can significantly reduce the stability of the structure, and concluded that non-critical loadings have the potential to cause yielding

in earthen structures (Quinn and Taylor 2013; 2014). In Oklahoma, the North Canadian Wastewater Levee and Arcadia Lake Dam, two of many U.S. Army Corps of Engineers (USACE)-owned assets, were identified for a case study of multi-hazard liabilities of earthen embankment structures. Upon entering documentation of hazards due to non-critical loadings for these structures into a geographic information system (GIS) database, numerous shallow earthquakes were noted to occur often within very close spatial and temporal proximity, as shown in Figure 1. Because the event clusters are associated with same shallow epicentral depth, defined as less than 10 km, and similar clusters were noted in other regions of historically low-seismic hazard throughout the Central United States, the initial study area was expanded beyond Oklahoma to include Arkansas, Kentucky, Missouri, Tennessee, Texas, and Virginia. These specific intraplate states were investigated due to the proximity of federal infrastructure, variable geology, and varying tectonic regimes, with the deliberate inclusion of both high hazard regions (New Madrid Seismic Zone [NMSZ]) and historically aseismic regions of minimal hazard.

Figure 1. Location of the North Canadian Wastewater Levee and Arcadia Lake Dam and proximity of seismic events greater than M2.0 from 01/01/2010 through 10/20/2013.

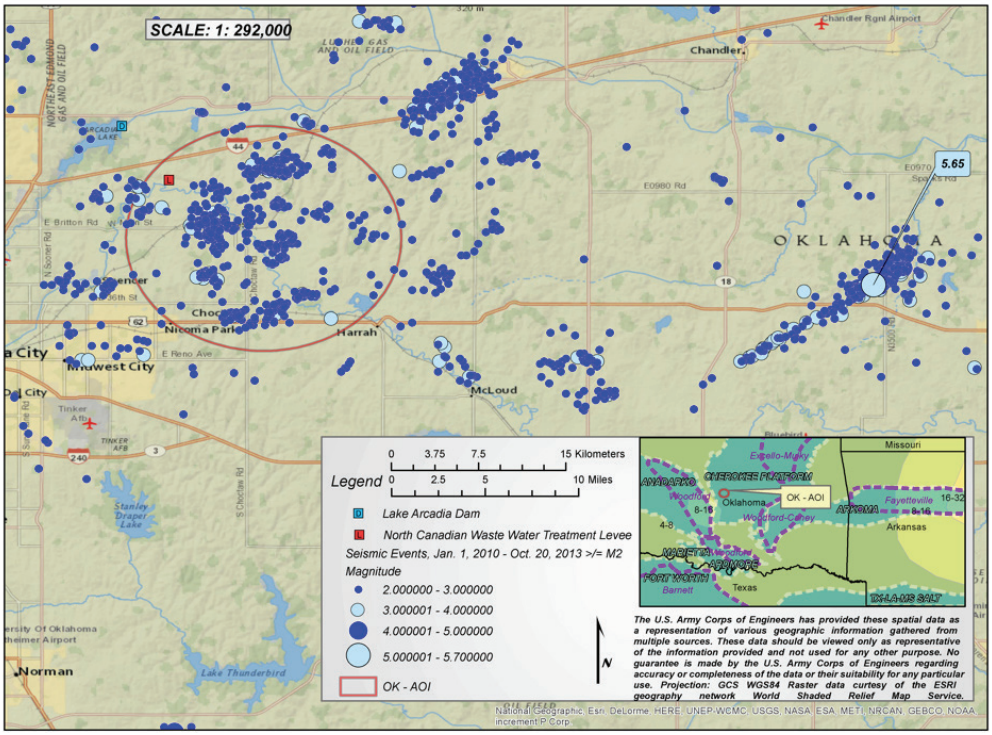

The seismic event database used in this investigation included complementary regional and national catalogs for their spatial coverage and instrumental sensitivity coverage (magnitude level) to generate a record of publicly reported seismological events that occurred from 02/08/1950 to 10/20/2013 for the seven-state study region (ANSS 2013; AGS 2013; CERI 2013; Frohlich and Davis 2002; NEIC 2013; SUSN 2013). A detailed account of how the seismic catalog was constructed can be found in the second technical report of this series ("Unconventional Hydrocarbon Development Induced Seismic Hazards Within the Central United States: Report 2, Seismological Data").

Sixty-three years (1950-2013) of data on reported **M**2.0 (**M** refers to reported magnitude) and greater earthquakes were analyzed for this intraplate study region. The analysis revealed a statistically significant increase (143%) in the number of seismic events was observed in the nine years from 2004-2013 as compared to the previous 54 years (Figure 2a). The magnitude scales, e.g., Moment Magnitude (M_w), Body Wave Magnitude (m_b), Surface Wave Magnitude (M_s), Richter Local Magnitude (M_L), etc., for the reported events between 1950-2013, vary significantly from the original magnitude scales proposed by Richter (1935) and Gutenberg (1945a; 1945b) due primarily to the technological advancements in seismometers and in an effort to apply the scales developed in southern California to other regions. Therefore, the magnitudes reported by different observatories contain some degree of bias and systematic differences. More than 100 different curves relating the different magnitude scales have been published with variable degrees of accuracy. It is beyond the scope of this research to identify which magnitude scale is most appropriate for accurately quantifying the radiated energy from geo-engineering activities in relation to Southern California tectonic events, which occur much deeper within the lithosphere. However, there is a small bias between different magnitude scale relations for natural events and M_w between relative magnitude range of 2 to 6 (Idriss 1985; Kramer 1996). The observation range, irrespective of magnitude scale, falls between magnitudes 2 and 6 within the Central United States; therefore, the term magnitude, **M**, used throughout this report is in reference to the reported magnitude scale of the reporting agency, wherein to a first order these scales are complementary. In reference to specific events or maximum potential predictions the magnitude scale is given as either the reported scale or moment magnitude, M_w, respectively.

Figure 2. Distribution of seismic events per decade in the study region and the temporal increase in unconventional hydrocarbon production wells. Since 2004, there has been a significant increase in not only the number of events but also in the observed magnitudes compared to the previous three decades (A); Event distributions of the past three decades indicating regional completeness at M2.0 and greater post-1974 (B).

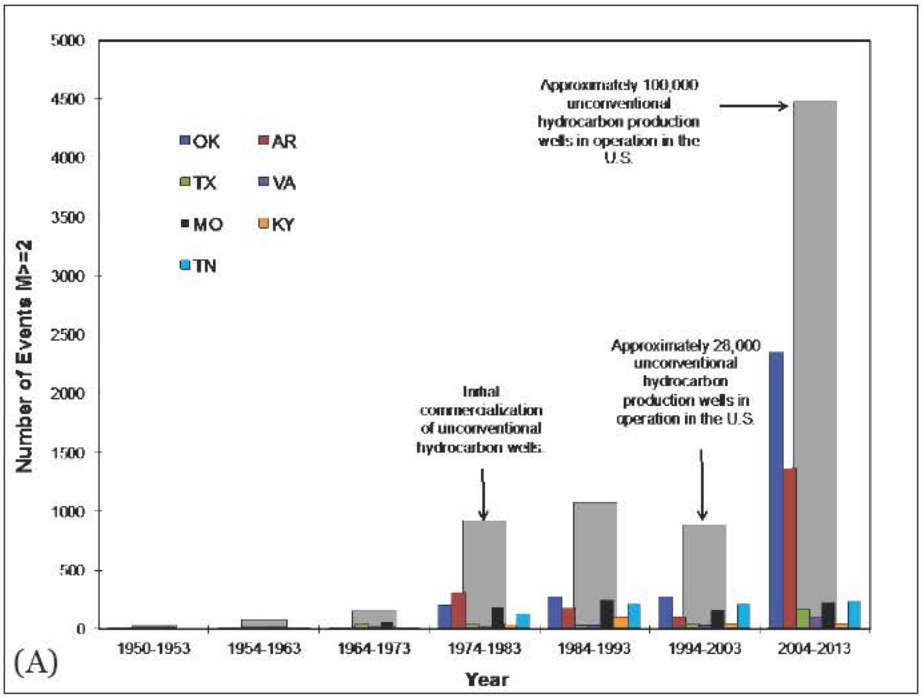

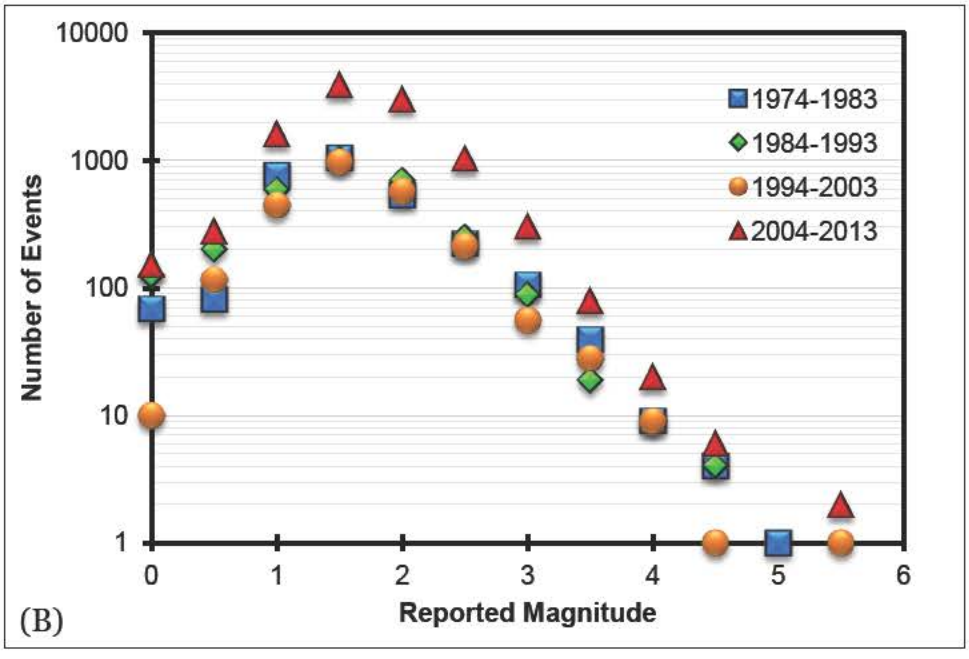

Prior to 1974, the instrument density and geospatial coverage was not adequate to develop a complete record of events throughout the study region at an accuracy of **M**2.0. However, post-1973, the distribution and frequency remained constant over each decade, despite advances in instrumentation, e.g., the EarthScope project (USArray 2014), with a catalog accuracy of **M**2.0, until 2004 when the observed spatial and temporal frequency increased, suggesting the possibility that the events were not solely tectonic in nature (Figure 2b and Tables 1 and 2). Additionally, post-2004 aseismic regions suddenly began experiencing seismic rates far in excess of those in high seismic hazard zones and at greater magnitudes not explainable by refinements in seismic instrumentation in the area.

The cumulative magnitude distribution of tectonic seismic events has been observed to follow the standard Gutenberg-Richter (G-R) relationship (Gutenberg and Richter 1944; 1949):

$$\log n(M) = a - bM \tag{2}$$

where *n(M)* is the cumulative number of events exceeding magnitude *M*, 10^a is the number of events exceeding the completeness threshold magnitude, and *b*-value describes the relative likelihood of small and large earthquakes. As the *b*-value increases, the number of large events decreases in comparison to small events; this does not necessarily mean that the physical quantity of large events decreases rather the ratio of large to small events decreases. The *b*-value is tectonically relatively static over region(s) of interest, ranging in value from 0.6-1.1 (Utsu 2002). Therefore, a stable *b*-value indicates the causality mechanism is relatively constant, e.g., tectonic plate theory, and that the small sampling of seismic observations, the past 100 years, are random time intervals of a larger geological process. A significant shift in *b*-value magnitude would indicate that an alternate source induction method is dominating a given region, and that the assumption of a constant process over time is not valid and must be identified to accurately assess the regional hazard and risk.

Table 1. Mean magnitude, b-values, and b-error values throughout the study region.

Completeness Magnitude	Spatial Region	Mean Earthquake Magnitude				b-value				b-error[2]			
		1950-2013	1950-1973	1974-2003	2004-2013	1950-2013	1950-1973	1974-2003	2004-2013	1950-2013	1950-1973	1974-2003	2004-2013
2.0	**SA[1]**	**2.43**	**3.20**	**2.44**	**2.39**	**0.898**	**N/A**	**0.892**	**0.995**	**0.01**	**N/A**	**0.02**	**0.01**
	AR	2.39	3.32	2.50	2.33	0.980	N/A	0.793	1.151	0.02	N/A	0.03	0.03
	KY	2.56	3.25	2.54	2.43	0.717	N/A	0.737	0.912	0.05	N/A	0.05	0.13
	MO	2.46	3.22	2.40	2.34	0.857	N/A	0.973	1.109	0.03	N/A	0.04	0.07
	OK	2.39	3.02	2.33	2.39	0.984	N/A	1.132	0.977	0.02	N/A	0.04	0.02
	TN	2.37	3.66	2.37	2.33	1.045	N/A	1.038	1.138	0.04	N/A	0.04	0.07
	TX	2.97	3.15	3.09	2.84	N/A	N/A	N/A	N/A	N/A	N/A	N/A	N/A
	VA	2.64	3.38	2.63	2.46	0.627	N/A	0.639	0.845	0.05	N/A	0.07	0.09
3.0	**SA**	**3.39**	**3.49**	**3.40**	**3.35**	**0.984**	**0.801**	**0.972**	**1.096**	**0.03**	**0.06**	**0.05**	**0.05**
	AR	3.44	3.47	3.45	3.41	0.890	0.843	0.871	0.935	0.07	0.18	0.09	0.11
	KY	3.47	3.32	3.50	3.54	0.841	1.180	0.786	0.736	0.12	0.36	0.13	0.33
	MO	3.44	3.54	3.35	3.45	0.889	0.734	1.079	0.869	0.08	0.11	0.14	0.25
	OK	3.32	3.56	3.32	3.29	1.180	0.717	1.167	1.268	0.07	0.14	0.17	0.08
	TN	3.31	3.88	3.27	3.30	1.218	0.470	1.364	1.241	0.14	0.23	0.18	0.31
	TX	3.41	3.44	3.41	3.39	0.947	0.891	0.943	0.989	0.08	0.16	0.12	0.13
	VA	3.56	3.44	3.62	3.69	0.712	0.893	0.650	0.585	0.10	0.19	0.16	0.16
3.7	**SA**	**4.07**	**4.10**	**4.05**	**4.07**	**1.034**	**0.965**	**1.073**	**1.042**	**0.07**	**0.14**	**0.12**	**0.13**
	AR	4.03	4.13	4.05	3.97	1.129	0.907	1.086	1.371	0.17	0.34	0.22	0.35
	KY	3.99	3.80	4.04	3.95	1.265	2.895	1.124	1.448	0.33	2.05	0.34	1.02
	MO	4.12	4.18	4.10	3.83	0.932	0.817	0.965	2.369	0.17	0.20	0.28	1.37
	OK	4.01	4.00	3.91	4.04	1.217	1.241	1.643	1.125	0.19	0.37	0.62	0.23
	TN	3.97	4.35	3.88	4.00	1.346	0.620	1.930	1.241	0.41	0.44	0.68	1.24
	TX	4.16	4.16	4.21	4.12	0.847	0.856	0.779	0.931	0.15	0.32	0.22	0.27
	VA	4.21	3.93	4.09	4.60	0.781	1.579	0.997	0.457	0.20	0.79	0.38	0.20

Note:

1. SA is the abbreviation for the seven state study region.

2. b-error is the standard error of the maximum predicted event from the Gutenberg-Richter Relation and does not represent "goodness" of b-value fit to the data.

3. The Completeness Magnitude is the magnitude for which the seismic record is complete based on instrument sensitivity to adequately detect and record all events of the corresponding magnitude and greater.

Table 2. Completeness record and rate throughout study region.

Completeness Magnitude	Spatial Region	∑N(m)3				Seismic Rates: ∑N(m)/yr			
		1950-2013	1950-1973	1974-2003	2004-2013	1950-2013	1950-1973	1974-2003	2004-2013
2.0	**SA[1]**	**7616**	**264**	**2869**	**4483**	**120.89**	**11.48**	**95.63**	**456.05**
	AR	1983	30	594	1359	31.48	1.30	19.80	138.25
	KY	249	13	190	46	3.95	0.57	6.33	4.68
	MO	883	80	579	224	14.02	3.48	19.30	22.79
	OK	3179	58	763	2358	50.46	2.52	25.43	239.88
	TN	802	5	560	237	12.73	0.22	18.67	24.11
	TX	328	54	109	165	5.21	2.35	3.63	16.79
	VA	192	24	74	94	3.05	1.04	2.47	9.56
3.0	**SA**	**950**	**165**	**374**	**411**	**15.08**	**7.17**	**12.47**	**41.81**
	AR	186	23	95	68	2.95	1.00	3.17	6.92
	KY	51	11	35	5	0.81	0.48	1.17	0.51
	MO	119	48	59	12	1.89	2.09	1.97	1.22
	OK	312	25	45	242	4.95	1.09	1.50	24.62
	TN	77	4	57	16	1.22	0.17	1.90	1.63
	TX	153	32	66	55	2.43	1.39	2.20	5.60
	VA	52	22	17	13	0.83	0.96	0.57	1.32
3.7	**SA**	**194**	**49**	**82**	**63**	**3.08**	**2.13**	**2.73**	**6.41**
	AR	46	7	24	15	0.73	0.30	0.80	1.53
	KY	15	2	11	2	0.24	0.09	0.37	0.20
	MO	31	16	12	3	0.49	0.70	0.40	0.31
	OK	43	11	7	25	0.68	0.48	0.23	2.54
	TN	11	2	8	1	0.17	0.09	0.27	0.10
	TX	32	7	13	12	0.51	0.30	0.43	1.22
	VA	16	4	7	5	0.25	0.17	0.23	0.51

Note:

1. SA is the abbreviation for the seven state study region.
2. ∑N(m) is the number of statistically relevant data points for a given Completeness Magnitude.
3. The Completeness Magnitude is the magnitude for which the seismic record is complete based on instrument sensitivity to adequately detect and record all events of the corresponding magnitude and greater.

A greater than 10% shift was observed in the **M**2.0 plus *b*-values, based on the Gutenberg-Richter Law, within the study region after 2004, shifting from 0.892 (1974-2003) to 0.995 (2004-2013) with a 477% increase in the rate of seismic events, **M**2.0 or greater, per year. Earthquake swarms and paleoseismic strains do not readily explain the causality shift observed in

either the *b*-value variance or the substantial rate increase, as those natural seismic events were observed in the 1974 to 2003 record with no significant influence on the regional *b*-values (Table 1). The same trends were observed for catalog accuracies of **M**3.0 and **M**3.7 and are explained in detail in the second technical report of this series ("Unconventional Hydrocarbon Development Induced Seismic Hazards Within the Central United States: Seismological Data"). Furthermore, areas of high seismic density were observed in regions that, pre-2004, had minimal to no reported seismic activity, nor did the areas include a significant known fault structure that would support such natural activity (Burchett et al. 1985).

Therefore, to understand and quantify the risk to infrastructure in these areas, a spatially and temporally correlated source of such activity, other than naturally occurring seismicity, needed to be identified. A common activity occurring across the states evaluated in this study and expansive enough to cause increased seismicity was geo-engineering activity, specifically unconventional hydrocarbon exploration and production. Changes in techniques for gas extraction and wastewater injection in relation to unconventional hydrocarbon production correlate well, both temporally with the increase in observed seismicity and spatially with the areas of recent high seismic density.

2 Unconventional Hydrocarbon Development Activity

2.1 History of North American shale gas production

From 1821 to 1974, shale gas exploration was in a state of infancy due to the relative ease of extraction and availability of coal and petroleum reserves. The first shale gas well was developed in 1821 at a depth of 21 m in the Devonian Dunkirk Shale (Appalachian Basin), which led to shale gas exploration and development extending throughout New York, Pennsylvania, Ohio, Kentucky, and Virginia (Curtis 2002; USDOE 2009). It was not until high-yield gas flow was achieved in the Devonian Ohio Shale (Appalachian Basin) in 1914 that commercialization of the world's first shale gas basin, the Appalachian Basin, occurred with the discovery of the Big Sand Gas Field (Zou 2013; Curtis 2002; USDOE 2009; Wang and Krupnick 2013; Roen 1993).

This renewed interest in shale gas, combined with technological advances in hydraulic fracturing, allowed for the exploration and development of commercially recoverable shale gas from the Mississippi System Barnett Shale (Fort Worth Basin) and produced the earliest boom in shale gas exploration (Zou 2013; Roen 1993). As a result, the Newark East Shale Gas Field, the largest gas field in the United States with recoverable reserves of approximately 7,400 x10^8 m^3, was discovered in 1982 and prompted further expansion of shale gas exploration and development from the Eastern United States to the Southern United States (Roen 1993). During the next 11 years, from late 1979 through 1990, U.S. shale gas production increased 2.5 fold (Wang and Krupnick 2013). This boom is observed within the seismic record, Figure 2a. Prior to 1974, seismic events of **M**2.0 and greater were relatively non-existent, based on “felt” intensity reports, but for the following three decades a significant increase is observed throughout the known shale gas-producing states of Oklahoma, Arkansas, Missouri, Kentucky, and Tennessee. Texas also recorded a significant increase in the preceding decade in the early 1970s, and this elevated seismicity remained relatively constant until 2004.

Over the following decade, from 1990 to 2000, shale gas was the primary target for U.S. gas development. Widespread expansion and production

occurred in the Ohio Shale (Appalachian Basin), Albany Shale (Illinois Basin), Barnett Shale (Fort Worth Basin), and the Lewis Shale (San Juan Basin) (Zou 2013; Wang and Krupnick 2013; Roen 1993). This wide-scale expansion of shale gas commercialization was due to technological and production advances within the industry, specifically: (i) drilling and well completion techniques, (ii) large-scale hydraulic fracturing, and (iii) gas pipeline construction. By the turn of the century, the number of shale gas wells reached 28,000 with annual production exceeding 100 $x10^8$ m^3 (Zou 2013; USDOE 2009). However, gas wells in this time period were still relatively shallow, vertical wells less than 1 km deep that posed minor induced seismic hazards (Figure 2).

By 2006, shale gas production had doubled to levels in excess of 200 $x10^8$ m^3 due to continual research and development advances in (i) horizontal well-drilling completion techniques and equipment, (ii) large-scale hydraulic fracturing practices, and (iii) the introduction of repetitive fracturing processes (Zou 2013). The most notable expansion occurred with the large-scale development of the Barnett Shale (Fort Worth Basin) that contained more than 1,000 production wells by 2001 with an annual gas production of 38.2 $x10^8$ m^3 (Zou 2013). By 2009, the Barnett Shale annual gas production of 100 $x10^8$ m^3 alone exceeded that of the entire North America production in the year 2000.

Since 2007, shale gas production has become a standardized process with large-scale research and development efforts in (i) horizontal well drilling and completion, (ii) large-scale hydraulic fracturing processes, (iii) refinements and improvements to repetitive fracturing techniques, and (iv) the synchronized fracturing of multiple wells. These technological improvements have exponentially accelerated shale gas commercialization, which accounted for 12% of the total North American gas production by 2009 (annual production of 930 $x10^8$ m^3 in the United States) (Zou 2013; USDOE 2009; Wang and Krupnick 2013; Roen 1993). Further, the presence of shale gas was confirmed in 46 sets of shale layers in more than 50 basins across the United States and Canada with an accumulated well total exceeding 100,000 by 2013 (Zou 2013; NRC 2013; Ellsworth 2013; USDOE 2009; Wang and Krupnick 2013). Horizontal drilling represents more than 75% of the total number of unconventional hydrocarbon wells per year with an annual average growth rate of 3,500-4,500 wells nationwide (Zou 2013) and lateral extents in excess of 3 km from the surface drill collar (NRC 2013).

More significantly, the average shale gas well depth increased from 180-2,000 m to 2,500-4,500 m with some wells exceeding 6,000 m in depth, subjecting the production and injection zones to significantly higher vertical/horizontal stress regimes (Zou 2013; NRC 2013). Therefore, these highly fractured zones generate larger extents of stress redistributions resulting in greater potential energy release from shear (slip) failure rockbursting for two reasons, (i) vertical wells do not yield the same extensive fractured rock zones as horizontal wells, thus the potential strain energy release is not as significant, and (ii) shallow horizontal wells are not as prone to rock failure from stress redistribution (CMRO 1988). As the fluid pressure decreases, the stresses redistribute, resulting in a delayed brittle failure within the rock mass (Turcotte et al. 2014).

2.2 Fracture development and basic characteristics of commercial shale

Shale gas is natural gas produced from the formation of organic-rich shale, typically in sedimentary basins. The shale play refers to the region of the shale basin in which the total organic content (TOC) is in excess of 2% in the gas generation window and the brittle mineral content is in excess of 40% (Zou 2013; USDOE 2009). Commercially viable shale plays should have an effective thickness of approximately 30 m; however, this can be less depending on the TOC. In North America, the maximum reported effective thickness is 304 m (Marcellus Shale Basin) while the minimum is 6 m (Fayetteville Shale Basin) (Zou 2013). However, the North American average effective thickness is in excess of 30 m (Zou 2013; USDOE 2009).

Commercially viable shale has a high brittle mineralogy that is easy to fracture; horizontal drilling is ideally conducted along the weakest principal stress axis, which is subjected to multiple hydraulic fractures to maximize the fractured zone extents in order to stimulate gas flow over the largest region possible, typically exceeding 30-50 m thickness (USDOE 2009; Zou 2013; NRC 2013).

The ideal shale for gas production should have low clay content, less than 30%, and high brittle mineral content, greater than 40%. The brittle mineral content is defined as the fraction of the shale mineralogy comprised of (i) quartz, (ii) calcite, and/or (iii) feldspar; an important factor that affects the shale pore matrix, microfracture development, gas bearing properties, and fracture stimulation (Zou 2013). There is no unique mineralogy for effective shales in North America. For example, the

Barnett Shale is rich in silica, while the Eagle Ford Shale is high in carbonate content. Under external forces, a high brittle mineral content allows for easier development of tree-network-shaped fractures, both naturally and from induced fracturing, and is therefore favorable for gas stimulation and production. Conversely, shale with high clay content has higher ductility, thus increasing the energy loss within the rock; i.e., requiring more imparted energy to generate fractures to increase permeability and stimulate gas flow. In the United States, the quartz content of gas-producing shale is between 28 to 52% with a carbonate content of 4 to 16%; thus, the typical brittle mineral content is 46 to 60% (Zou 2013).

Since the early 2000s, the full extents of the fracture zones can be monitored through microseismic fracture mapping (Wang and Krupnick 2013). The full extents of the fractures are regarded as proprietary information; however, the end result is large zones of fractured rock, as thick as 50 m or more, with lateral extents of up to 3 km and at an average well depth of 4 km.

2.3 Correlation between unconventional hydrocarbon development and conventional mining

Mining is defined as the extraction of geological minerals, such as metals, coal, and oil shale, which cannot be grown through agricultural processes or created artificially in a laboratory or factory. This includes the extraction of non-renewable resources, e.g., petroleum and natural gas. The term “conventional mining” is used throughout this paper to describe deep ore mining processes wherein human activity occurs within the mining tunnels or stopes to excavate and extract the resource. In unconventional hydrocarbon development, the energy release associated with process of hydraulic fracturing is similar to blasting activities used in conventional mining. In the petroleum and natural gas industry, the term “fracing” refers specifically to the hydraulic fracturing of gas or oil source rock. Outside the industry, the term is commonly, and incorrectly, used to describe all parts of the unconventional hydrocarbon development process. However, hydraulic fracturing is only one component of shale gas production. Hydraulic fracturing is the process used to increase the permeability of the formation containing recoverable hydrocarbons. Hydraulic fracturing utilizes highly pressurized fluid (usually water) containing various chemicals and particulate solids (generally silica sand) to fracture the rock (Zou 2013; NRC 2013). The solids in the fluid are

called proppant, and they are forced into the fractures, which 'props' them open. The hydraulic fracturing process creates a highly permeable zone adjacent to the well casing, allowing for the flow of gas back to the surface. In areas where it is permissible, injection wells are also used to stimulate gas flow for repetitive and multi-stage fracturing and/or disposal of wastewater associated with unconventional hydrocarbon production (Zou 2013; NRC 2013). While waste fluid injection is typically located above or below the producing gas or oil horizon, it has been documented to contribute to induced seismicity (NRC 2013).

Mining introduces a cavity, or relative void, within the rock mass in which the previously stable stress state is disturbed and stresses are reoriented at a distance of up to a few times the cavity length (Cook 1976; Yerkes and Castle 1976; McClain 1970; Cranswick 2011). This stress redistribution, measured in terms of stress drops or strain energy release, can cause fault slips, shear failures along geological discontinuities, and/or rock failure; i.e., induced earthquakes or "rockbursts" (Kisslinger 1976; Cook 1976; Yerkes and Castle 1976; McClain 1970; Martin 1972; Cranswick 2011). While some rockbursts occur along mining walls or stopes, e.g., pillar failures, abutment failures, and face burst, these rockbursts typically yield induced events of M3.0 and less (Lenhardt 1988). The more significant events, greater than M3.0, are associated with fault or geological discontinuity failures (Lenhardt 1988). This phenomenon has been extensively researched in the deep, laterally extensive gold mines of South Africa for over 50 years (Cook 1976; Ortlepp 2005; Cook 1964; Spottiswoode and McGarr 1975). Furthermore, it is well-documented that human activities related to mining practices, whether surface or underground mining, extraction of fluid or gas or subsurface fluid injection/reinjection, are capable of causing seismic events, in some cases in excess of **M**5.0 (NRC 2013; Kisslinger 1976; Cook 1976; Yerkes and Castle 1976; McClain 1970; Ortlepp 2005; Cranswick 2011; Cook 1964; Spottiswoode and McGarr 1975; Gibowicz and Kijko 1994; Ellsworth 2013; McGarr 2014).

In unconventional hydrocarbon development, the process of hydraulic fracturing is not too dissimilar from blasting activities in conventional mining in terms of compressional seismic energy imparted into the rock mass. The rock mass is fractured, by either method, through the compressional pressures of a propellant, e.g., an explosive compound, such as ANFO (ammonium nitrate fuel oil), or highly pressurized fluid. The resultant seismic magnitude is therefore limited by the propellant

pressures rather than accumulated energy release of the rock (i.e., the larger the explosion the greater the equivalent earthquake.) Furthermore, compressional energy releases yield a different seismic signature than tectonic rupture. However, for all mining purposes, conventional or unconventional, the "blasting" activities are microseismic and rarely exceed **M**2.0 (NRC 2013; Ellsworth 2013; Richardson and Jordan 2002; Ortlepp et al. 2005) and do impart stress drops into the rock mass.

For wastewater injection wells, the pressurized fluid will maintain a time-dependent stability within the rock mass until such point where the pore pressures dissipate, through hydraulic conductivity and diffusion, and the stress regime is again redistributed and prone to failure (Kisslinger 1976; McGarr 2014; Horton 2012; Frohlich et al. 2011). Additionally the added fluid mass will increase the stresses to the rock mass and can by itself generate induced seismicity, similar to reservoir impoundment (Kisslinger 1976; Cook 1976; Yerkes and Castle 1976). Thus, the combination of fluid pressurization, decrease of effective stresses, pore pressure dissipation, and mass increase would make wastewater injection the largest singular contributor to induced seismicity. Other unconventional hydrocarbon production components such as fluid/gas extraction are known to cause induced seismicity through stress redistribution and the creation of subsurface voids (Yerkes and Castle 1976; Maury et al. 1976).

As all components of unconventional hydrocarbon development can yield stress redistributions within the rock mass, it is not always possible to definitively determine which activity produced the stress drop that caused failure within the rock mass or slip along a fault. Therefore, no one component of unconventional hydrocarbon development is singled out as a causality mechanism. Rather, the sum of all unconventional hydrocarbon development activity is considered to contribute to the induced seismicity or rockbursts.

3 Induced Seismicity from Unconventional Hydrocarbon Production

3.1 Comparison to rockbursts and other failure mechanisms

Initially theorized in the 1976 *Engineering Geology* special issue on induced seismicity, underground explosions, specifically for the stimulation of trapped hydrocarbons, have the potential to induce significant seismicity in highly pre-stressed rock. For wastewater injection wells, the pressurized fluid will maintain a time-dependent stability within the rock mass until such point where the pore pressures dissipate, through hydraulic conductivity and diffusion, and the stress regime is again redistributed and prone to failure (Kisslinger 1976; McGarr 2014; Horton 2012; Frohlich et al. 2011). Additionally, the added fluid mass will increase the stresses to the rock mass and can by itself generate induced seismicity similar to reservoir impoundment (Kisslinger 1976; Cook 1976; Yerkes and Castle 1976). Thus, the combination of fluid pressurization, decrease of effective stresses, pore pressure dissipation, and mass increase would make wastewater injection the largest single contributor to induced seismicity. Keranen et al. (2013) proposed that the Prague, OK, 2011 **M**5.0 foreshock, **M**5.7 mainshock, **M**5.0 aftershock sequence was triggered by wastewater injection. Based on volume of injected fluid, McGarr (2014) illustrates that wastewater injection alone does not yield sufficient strain energy release to account for all the seismic moment required. However, both hypotheses neglect any contributions from the vast number of unconventional hydrocarbon production wells near both the disposal wells and epicentral area. Individually, the wells may not contribute significantly to the overall seismic potential, but the accumulative energy from the well systems tapping into the same geologic formation could produce sufficient seismic moment to account for the sequence theorized by Keranen et al. (2013).

Fluid injection into low permeability rock (shale) can cause rock fracturing due to increases in pore pressure and brittle fracturing due to stress corrosion, both of which can induce seismicity (Zou 2013; NRC 2013; Ellsworth 2013; Keranen et al. 2013; McGarr 2014). Additionally, laboratory investigations showed that an increase of water in quartz, the predominant brittle mineralogy in shale, dramatically increases fracture growth and significantly decreases the time to failure (Kisslinger 1976;

Cook 1976; Yerkes and Castle 1976; Maury et al. 1976; McClain 1970; Martin 1972; Scholtz 1972). Until recently, neither the theoretical nor laboratory causality modes were observed on a mass scale, because research focused on single triggering mechanisms and localized areas. These predicted triggers all are components of current unconventional hydrocarbon development; thus, no individual component should be singled out since it is the net summation of several process components (hydraulic fracturing, injection, extraction, and re-injection) that contribute to the weakening and fracturing of the subsurface, stress redistribution, and subsequently may result in induced seismicity.

In either conventional mining or unconventional hydrocarbon development, the end result is the same; zones of highly fractured rock are generated wherein the fracturing causes a stress drop, or redistribution, throughout the surrounding rock mass that can potentially generate induced seismicity. The geological structure critically influences location, magnitude, and nature of induced seismicity and not all mining operations will generate seismic activity (Kisslinger 1976; Cook 1976; Yerkes and Castle 1976; McClain 1970; Ortlepp 2005). Unfortunately, the current state of knowledge does not allow prediction of which formations, conditions, and activities make one site more susceptible to inducement of seismicity than another. Thus, not all unconventional hydrocarbon development will induce seismicity, where one region may experience less induced seismicity than another even at equal or higher gas production rates. Prior to any geo-engineering activities, the rock mass is in a relative state of equilibrium with some portions critically close to failure depending on the vertical and horizontal compressive stress regime (Kisslinger 1976; Cook 1976; Yerkes and Castle 1976; Maury et al. 1976; McClain 1970; Cranswick 2011). For an aseismic region, the rock mass remains in this meta-stable state unless acted upon by an outside force, e.g., geo-engineering activities such as drilling, injection, and mining. In the early 2000s, shale gas became commercially viable with advances in equipment and directional drilling. Being able to drill horizontally exposed more of the hydrocarbon rich formation to the well and presented significant efficiency over the vertical wells that had previously been the industry standard. This significant advance in unconventional hydrocarbon development yields higher recoveries over much larger regions. However, this advance in shale gas recovery also results in higher volumes of waste fluid that is re-injected into the subsurface and larger

expanses of hydraulically fractured and weakened rock mass. Both of these factors can contribute to subsurface failures, or rockbursts.

"Rockburst," as a general term related to the generation of induced-seismic events, is the sudden violent rock failure caused by the release of accumulated energy when a rock mass is strained beyond the elastic limit. Rockbursts can be classified as strain, crush, or slip bursts; strain bursts are small and localized, while slip and crush bursts are larger and can cause extensive damage (Cook 1976; Ortlepp 2005; Cranswick 2011; Lenhardt 1988; Scott et al. 1997; Bennett and McLaughlin 1997). Rockbursting need not occur along the longwall rockface or stope abutment. Rather, the more serious rockbursts occur along faults and/or geological discontinuities within the rock mass within proximity to mining activity (Ortlepp 2005; Lenhardt 1988; Bennett and McLaughlin 1997). The prevailing assumption in unconventional hydrocarbon production-induced seismicity is that fault movement is the only mechanism of energy release large enough to generate "felt" seismic events, whether from currently active faults or rejuvenation of ancient dormant faults (NRC 2013; Kisslinger 1976; Cook 1976; Yerkes and Castle 1976; McClain 1970; Ortlepp 2005; Cranswick 2011; Cook 1964; Spottiswoode and McGarr 1975; Gibowicz and Kijko 1994; McGarr 2014; Horton 2012; Frohlich et al. 2011). However, unconventional hydrocarbon production also has the potential to generate rockbursts within the subsurface, be it slip along a geological discontinuity, shearing of pristine rock, or activation of an intersecting or nearby tectonic fault dependant on the geological conditions and stress redistribution from the unconventional hydrocarbon production activities. Bennett and McLaughlin (1997) analyzed the two largest mining-induced earthquakes observed before 1997 and concluded that the failure mechanisms were highly implosional; gravitational energy released by the collapse of the undermined rock mass was sufficient to account for all the released seismic energy. Therefore, tectonic involvement was neither necessary nor expected in either instance. As such, rockbursts can produce tectonically analogous "earthquakes" in aseismic continental regions without faults or surface traces; thus, quantifying the hazard potential from unconventional hydrocarbon development-induced seismicity is both complex and problematic.

The more violent events associated with rockbursts range in magnitude from **M**2.0 to **M**5.0, while the blasting activities, i.e., intentional fracturing of the rockface, are typically less than **M**1.0 but can reach up to

M2.0 and are readily differentiated seismically (NRC 2013; Ortlepp 2005; Ellsworth 2013; Richardson and Jordan 2002). Rockbursts have been documented worldwide for nearly a century. In the South African gold mines, which can reach depths in excess of 3,500 m with up to 800 km of subsurface tunnels, the rockbursting phenomenon is exacerbated in that several contiguous mines exploit a single continuous ore body (Cook 1976; Ortlepp 2005; Cranswick 2011; Bennett and McLaughlin 1997; Cook 1964; Spottiswoode and McGarr 1975; Notley 1983; Kaneko et al. 1990; Krishnamurthy and Shringarputale 1990; Dunlop and Gaete 1997; Li and Guo 2001; Båth 1984; CMRO 1988). In this case, large areas of the earth's crust are effectively weakened and stresses within the rock are redistributed by mining operations, a similarity observed in current unconventional hydrocarbon production within the Central United States at depths exceeding 2000m (Kisslinger 1976; Cook 1976; Maury et al. 1976; McGarr 2014; Horton 2012; Frohlich et al. 2011).

Rockbursts are not unique to South African gold mines and have been observed in conventional mining activities throughout Canada, Australia, Japan, India, Chile, China, United States, and Western Europe (Ortlepp 2005; Cranswick 2011; Bennett and McLaughlin 1997; Notley 1983; Kaneko et al. 1990; Krishnamurthy and Shringarputale 1990; Dunlop and Gaete 1997; Li and Guo 2001; Båth 1984). Large shear fractures, 30-m vertical by 100-m longitudinal, with shear displacements of a few centimeters have been observed in conventional mining; these dimensions yield a potential seismic moment on the order of 5,000 GJ associative with **M**2.0 earthquakes (Cook 1976). The process of hydraulic fracturing, combined with extensive horizontal drilling, has the potential for the development of shear fractures with longitudinal components of up to two orders of magnitude greater than previously described along a single directional axis. Thus, the seismic moment potential and associative seismic hazard is significantly increased.

Usually rockbursts occur along known geological faults or geological dikes. On rare occasions, the slip movement is visible within the mine. However, most often the slip surface is not exposed, and the failure mechanism is assumed through seismological data and known geologic structure. While less frequent, rockbursts occur due to a sudden shear fracture through pristine rock where no faults or pre-existing discernible planar weaknesses exist. These dynamic brittle shear zones have been observed in several mine-induced seismic events and studied extensively since the 1970s

(Ortlepp et al. 2005; Gay and Ortlepp 1978; Ortlepp 1992; Ortlepp 2001; Ortlepp et al. 2004). These dynamic brittle zone failures, as a source mechanism, have the potential for generating a more violent energy release than fault-related slip (Ortlepp et al. 2005; Ortlepp 2001). The release of strain energy from rockbursts, in terms of seismic radiation, is analogous to tectonic fault slip, suggesting that South African gold mines can be used as an earthquake laboratory (Ortlepp 2005; Richardson and Jordan 2002; Ogasawara et al. 2002; McGarr et al. 2009).

Wastewater injection has been correlated to some of the larger observed induced seismic events, including the 2011 M_w 5.7 Oklahoma event (NRC 2013; Yerkes and Castle 1976, Ellsworth 2013; McGarr 2014; Horton 2012; Frohlich et al. 2011; Keranen et al. 2013). Moreover, there exists a probability that unconventional hydrocarbon development-induced seismic events are falsely attributed to neotectonic behavior rather than induced-seismicity: there is no current strictly seismological analysis to discriminate between tectonic fault slip and rockbursting (Ortlepp 2005; Ellsworth 2013; Richardson and Jordan 2002; Ortlepp et al. 2005; Gay and Ortlepp 1978; Ortlepp 1992; Ortlepp 2001; Ortlepp et al. 2004; Ogasawara et al. 2002; McGarr et al. 2009).

3.2 Correlation of unconventional hydrocarbon production with observed seismicity increase within the Central United States

The exponential rise in unconventional hydrocarbon production in the Central United States has correlated spatially and temporally with a rise in seismicity that cannot be attributed simply to tectonic activities (Hough et al. 2003). To differentiate between neotectonic and induced seismicity, a thorough GIS analysis was performed using the Ortlepp 30-km criterion (Ortlepp 2005). This criterion was developed from the distribution of seismic events in the Kaap-Vaal craton in South Africa, a highly stable intraplate seismic region with relatively no natural events prior to mining activities (Ortlepp 2005; Cranswick 2011). Events within the 30-km buffer could be geospatially associated with mining activity, where additional research has shown that the epicentral location of induced seismicity from geo-engineering activities can also be typically constrained by a 30-km buffer (Klose 2010). The Ortlepp 30-km criterion has been applied in more depth to mining-induced seismicity in Australia, where it was concluded that it is conservatively biased towards larger magnitude events, e.g., the **M**6.7 Tennant Creek event, where only a third of the aftershock zone was encompassed by the 30-km buffer (Cranswick 2011). However, within the

Central United States only the 2011 M_w5.7 Oklahoma event would be of sufficient size to be affected by the large magnitude bias of the 30-km criterion (Keranen et al. 2013). In this study, the Ortlepp 30-km criterion was applied conservatively to the centroid of 2.56 km² GIS cells that contained at least one known unconventional hydrocarbon production well vertical collar. The seismic record was analyzed for all seismic events greater than or equal to **M**2.0 to exclude any potential bias associated with active fracturing activities, i.e. compressional energy release. A complete detailed account of the GIS framework, methodology and analysis can be found in the third technical report of this series ("Unconventional Hydrocarbon Development Induced Seismic Hazards Within the Central United States: Report 3, Analytical GIS Methodology").

From 1950 to 2013, the entire study region has reported 7,616 seismic events greater than or equal to **M**2.0 (Table 3). Furthermore, the spatial epicentral distribution, especially of the past decade, follows the contours of shale basins and published effective shale plays as opposed to known faults (Figures 3 and 4). The exception is the distribution within the NMSZ in Figure 3. However, the "high seismic hazard" of the NMSZ accounts for only 16.4% (1,247 events) of reported events since 1950. Prior to the shale gas production boom in 2004, the NMSZ accounted for 29.0% of the seismicity within the study region; however, it now accounts for only 7.5% of the reported seismicity over the past decade. Contrastingly, 58.8% of all reported events since 1950 have occurred within the last decade. Of these events, 83.9% have epicentral locations within 30 km of at least one known unconventional hydrocarbon production well vertical collar, shown in Table 3 and Figure 4. Thus, the shale gas production regions are 11 times more seismically active than the entirety of the high-hazard NMSZ for the record period from 2004 through 2013. Furthermore, the tectonic regime within the shale gas production zones, shown in Figures 3 and 4, does not have the tectonic fault structure to support the size and frequency of observed events (Burchett et al. 1985).

Table 3. Breakdown of publicly reported seismic events within the study region.

	02/08/1950 to 10/20/2013		01/02/2004 to 10/20/2013		01/02/2004 to 10/20/2013 within 30-km Buffer	
	All Magnitudes	M2.0+	All Magnitudes	M2.0+	All Magnitudes	M2.0+
Regional	19098	7616	10454	4483	7857	3769
Arkansas	3572	1983	2438	1359	2168	1219
Kentucky	599	249	89	46	29	25
Missouri	3552	883	1094	224	0	0
Oklahoma	7145	3179	5429	2358	5429	2358
Tennessee	3570	802	1119	237	67	23
Texas	333	328	165	165	111	111
Virginia	327	192	120	94	10	10

	01/02/2004 to 10/20/2013 within 30-km Buffer		Period Of Peak Seismic Activity Since 02/08/1950		
	All Magnitudes	M2.0+	Dates	M2.0+	% Of Total Events
AOI - OK	1673	594	01/01/2010 - 09/07/2013	566	95.29%
AOI -AR	1659	870	02/17/2010 - 10/28/2011	850	87.27%
Combined AOI AR & OK	3332	1464			

Figure 3. Study region with shale basins, effective shale plays, known faults 5 km or greater in length, Quaternary faults, and reported seismic activity, M2.0 or greater, since 01/02/2004.

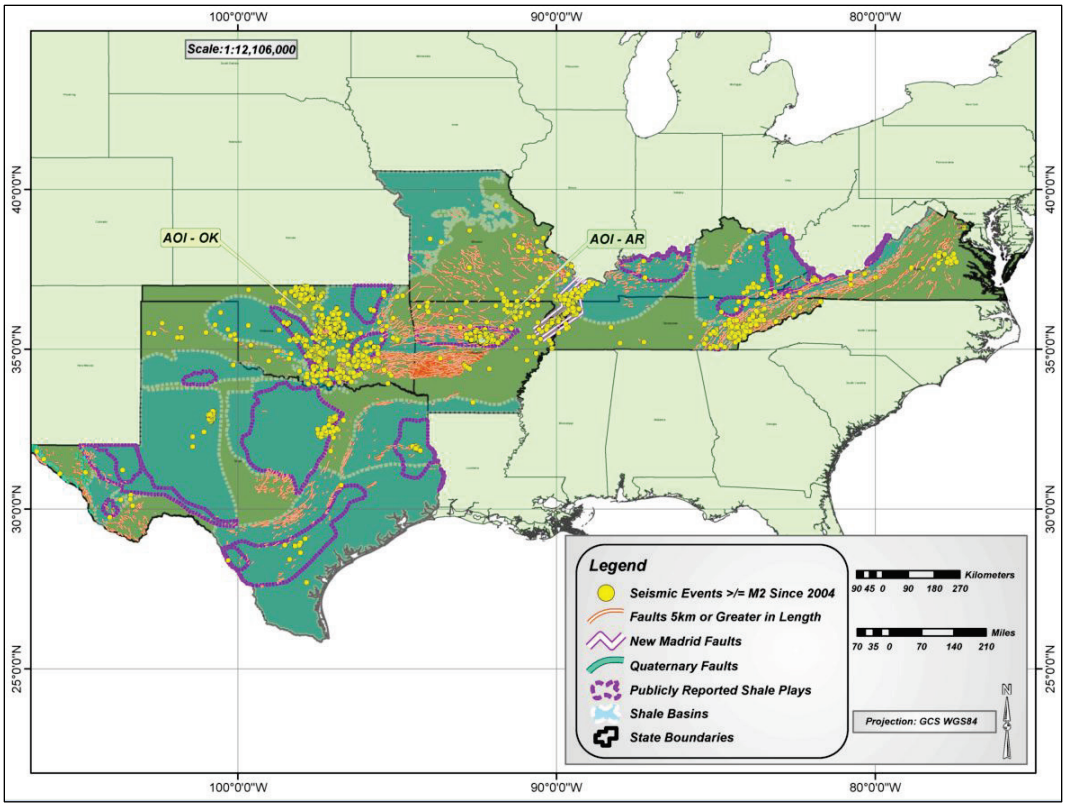

Within the past decade, 32.7% of all the seismic events have occurred within two 112 km² regions, i.e., Oklahoma (AOI-OK) and Arkansas (AOI-AR), as seen in Figure 4. Since 1950, the first reported seismic event for the AOI-OK occurred 31 March 2006. Since then, 1,673 events have occurred through 20 September 2013; 35.5% were **M**2.0 or greater. Similarly, since 1950, in AOI-AR, 974 events **M**2.0 or greater have been reported, wherein 87.3% of these events occurred during a 20-month period between 17 February 2010 and 28 September 2011. All these seismic events occurred within 10 km of at least one known shale gas production well vertical collar. This illustrates that little to no seismicity was reported within these areas prior to gas production, and this region is now more seismically active after shale gas commercialization than the entire NMSZ.

Figure 4. The seismic event density since 2004, for all seismic events M2.0 or greater throughout the study region focusing on Oklahoma and Arkansas (including the NMSZ), in relation to publicly reported effective shale plays and known faults in excess of 5 km in length. Callouts, AOI-OK and AOI-AR, indicate 112 km2 areas of greatest event density (AOI-OK = 594 events; AOI-AR = 870 events).

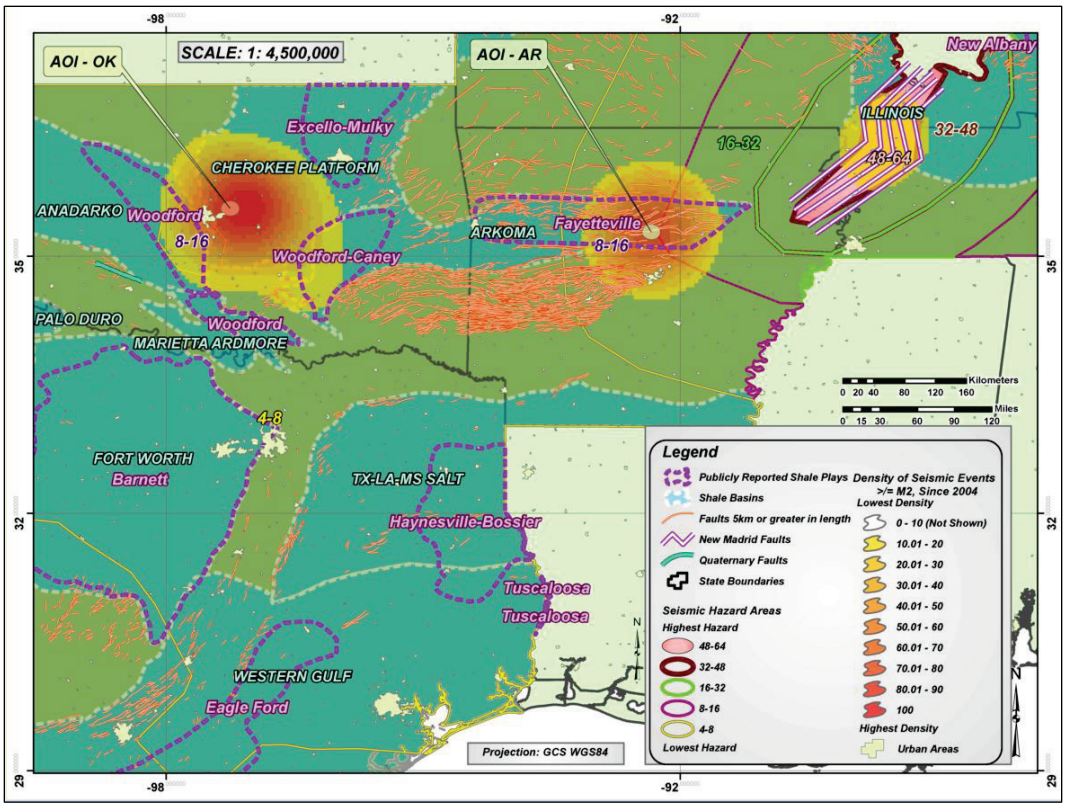

As an example, the development of the Fayetteville Shale (Arkoma Basin) gas reserves began in 2004, with the completion of more than 2,000 wells within five years, and is one of the ten largest gas plays in the United States (Zou 2013; NRC 2013; USDOE 2009). Prior to 2004, the Fayetteville Shale play averaged approximately 12 seismic events **M**2.0 or greater per year over a 54-year period from 8 February 1950 to 2 January 2004. After 2004, the seismic rate increased to 121 seismic events **M**2.0 or greater per year with 72% of these clustered within a 112.3 km² region. Moreover, all of the post-2004 events occurred within 30 km of at least one known unconventional hydrocarbon production vertical well collar.

While there is a significant amount of faulted structure in the AOI-AR that could explain the presence of earthquakes, it is the complete opposite situation for the AOI-OK. There is insufficient fault structure in the AOI-OK (fault system of 5 km or greater) to support this degree of activity at this concentration within the regions of highest seismic density (Figure 5).

Applying a 1 km radial buffer to reported fault systems of 5 km, or greater in length, only 21.4% of the **M**2.0 or greater events, throughout the 7-state region, within the 30-km Ortlepp buffer occurred on or near known faults. It must be noted that 100% of the seismic activity occurred at least 5 km outside of the 1-km fault buffer zone within the AOI-OK. While faults of less than 5 km exist within the study region, they were excluded from this analysis unless part of a larger fault system in excess of 5 km, as there are documented horizontal wells at the same depths that are greater in length and would have more seismic potential. There are no reported faults of any size within the AOI-OK, the region of second highest seismic density within the entire study region. This observation is in contrast to the prevailing assumption that wastewater injection intersecting a fault system is the genesis of induced seismicity and lends credibility to the hypothesis that rockbursts, e.g., geological discontinuity failure between two rock formations, can be responsible for significant seismicity.

Over a nine-year period (2004-2013), the combined seismic density of AOI-AR and AOI-OK, a total area of 224 km², is approximately 6.5 events per km² at a rate of about 146 events per year. Contrastingly, the NMSZ, which is considered the highest region of seismic hazard in the Eastern and Central United States, has a seismic density of approximately 0.02 events per km² at an average rate of 34 events per year. Additionally, the NMSZ's highest seismic rate occurred in 1984, with 55 events that year of **M**2.0 or greater, and is significantly less than either the AOI-OK or AOI-AR regions. Figures 3 and 4 illustrate the seismic density discrepancy between events attributed to unconventional hydrocarbon production and intraplate tectonics. Furthermore, the largest event reported in the NMSZ since 1950 is the 1976 m_b 4.9 event (Intensity VI), whereas the maximum reported event in the shale gas production regions was the 2011 M_w 5.7 Oklahoma event (Intensity VIII), as shown in Table 4. Therefore, the seismic hazard associated with unconventional hydrocarbon development is more frequent and more concentrated than in previously established high hazard zones (Figure 4). Moreover, outside of the NMSZ, infrastructure is not designed to accommodate such hazards (USACE 1970a; USACE 1995; USACE 1970b; USACE 1997; USACE 2014a; USACE 2014b; USACE 2014c; Yegian et al. 1991).

Figure 5. The epicentral proximity to reported fault systems since 2004, for all seismic events M2.0 or greater throughout the study region focusing on AOI-OK. Faults shown in inset are from USGS (2013a; 2013b); Burchett et al. (1985) and Gay (2003).

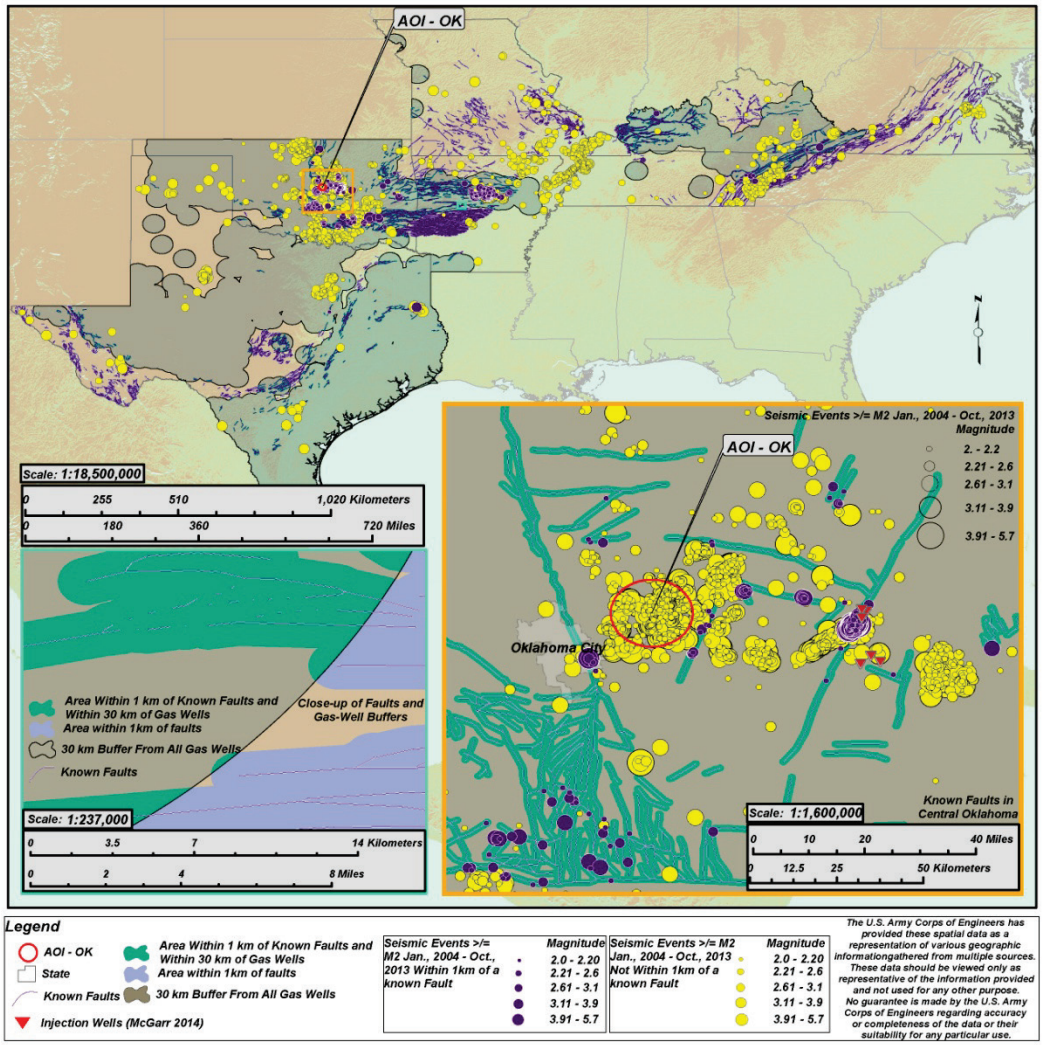

Table 4. List of largest magnitude events and nearby dams or levees.

Magnitude	State	Lat.	Lon.	Depth (km)	Dam / Levee (D/L)	Distance (km)	Date
A. M_L 4	OK	35.468	-97.345	2.9	L: North Canadian Wastewater Treatment Levee (NCWWT) D: ARCADIA LAKE DAM	14.5 19.6	02/27/13
B. m_b 4	OK	34.635	-95.875	5.0	L: Cumberland Levee; D: SARDIS LAKE DAM	86.6 48.1	04/03/12
C. M_L 4	OK	35.519	-96.784	5.0	L: NCWWT Levee D: ARCADIA LAKE DAM	47.9 53.9	11/06/11
D. M_{bLg} 4.1	TX	31.844	-94.3	5.0	D: FERRELLS BRIDGE DAM D: SAM RAYBURN DAM	103.8 83.2	01/25/13
E. M_w 4.1	OK	35.535	-96.757	3.7	L: NCWWT Levee D: ARCADIA LAKE DAM	50.2 56.1	02/27/10
F. M_w 4.1	AR	35.304	-92.317	4.9	L: Conway County Levee No. 8	30.0	10/11/10
G. M_w 4.1	AR	35.272	-92.378	6.2	L: Conway County Levee No. 8	23.6	02/18/11
H. m_{wr} 4.2	TX	31.966	-94.526	4.7	D: FERRELLS BRIDGE DAM; D: SAM RAYBURN DAM	88.6 107.6	09/02/13
I. M_w 4.2	OK	35.681	-97.098	7.0	L: NCWWT Levee D: ARCADIA LAKE DAM	20.8 24.2	04/16/13
J. M_w 4.2	KY	37.139	-83.054	17.0	D: CARR CREEK LAKE DAM	9.3	11/10/12
K. m_b 4.3	VA	37.2	-81.92	1.0	D: FISHTRAP DAM (Kentucky); D: JOHN W FLANNAGAN DAM	51.0 37.5	11/02/06
L. m_b 4.3	VA	37.157	-81.975	NA	D: FISHTRAP DAM (Kentucky); D: JOHN W FLANNAGAN DAM	49.6 33.9	11/23/06
M. m_{wr} 4.3	TX	31.91	-94.428	4.7	D: FERRELLS BRIDGE DAM; D: SAM RAYBURN DAM	95.0 98.6	09/02/13
N. M_w 4.35	OK	35.176	-97.321	3.1	L: NCWWT Levee D: ARCADIA LAKE DAM	46.9 52.2	10/13/10
O. M_w 4.4	OK	35.686	-97.089	6.2	L: NCWWT Levee D: ARCADIA LAKE DAM	21.8 25.0	04/16/13
P. M_w 4.7	AR	35.269	-92.355	3.2	L: Conway County Levee No. 8	24.9	02/28/11
Q. m_{wr} 4.8	TX	28.865	-98.079	5.0	L: Three Rivers Local Flood Protection	43.3	10/20/11
R. m_{wr} 4.8	TX	31.926	-94.369	5.0	D: FERRELLS BRIDGE DAM; D: SAM RAYBURN DAM	93.8 98.6	05/17/12
S. M_w 4.9	OK	35.534	-96.766	3.4	L: NCWWT Levee D: ARCADIA LAKE DAM	49.3 55.3	11/05/11
T. M_w 4.9	OK	35.519	-96.792	2.5	L: NCWWT Levee D: ARCADIA LAKE DAM	47.4 53.4	11/08/11
U. M_w 5.65	OK	35.522	-96.78	3.1	L: NCWWT Levee D: ARCADIA LAKE DAM	48.5 54.4	11/06/11

4 Induced Seismic Hazard and Risk Potential

The *hazards* associated with rockbursts have been well documented in over 50 years of research wherein high accelerations were observed at relatively shallow depths compared with neotectonic events (Cook 1976; Ortlepp 2005; Lenhardt 1988; Bennett and McLaughlin 1997; Krishnamurthy and Shringarputale 1990; Ortlepp 2001; McGarr 1971; McGarr 1984; Lenhardt 1990; Lenhardt 1992). In the United States, rockbursts associated with conventional mining have been documented since the 1930s in the Coeur d'Alene mining district in Idaho (Bolstad 1990). Additional rockburst cases within the United States have also been reported, e.g., the 30 rockburst events between **M**3.0 to **M**3.8 over 35 years in the Wasatch Basin in Utah and the 19 events recorded over two years, from **M**2.3 to **M**4.3, in a single coal mine in Kentucky (Ortlepp 2005; Bennett and McLaughlin 1997). As such, rockbursting is not a new phenomenon or *hazard* to the United States and this study region. Figures 2, 3, and 4 illustrate that there is a significant *hazard*, in terms of an increasing trend in both event magnitude and frequency, associated with induced seismicity related to unconventional hydrocarbon development. Furthermore, research within USACE has shown that non-extreme loadings from multiple hazards, including low peak ground accelerations associated with small magnitude events of **M**3.0 to **M**5.0, can yield critical combinations that can potentially cause straining and/or failure within earthen embankments (Quinn and Taylor 2013; 2014). There have been documented cases where repetitive, low-amplitude seismic impulses, e.g., pile driving activities, led to structural failures even though the surface wave amplitudes were well below the established threshold for extremely sensitive structures (Bradshaw et al. 2007; Baxter et al. 2013; Davis 2004; Taylor 2011).

A single microseismic event, less than **M**3.0, poses little structural *risk* and is often ignored. However, the significant increase in observed microseismic events since 2004, compared to the three previous decades (Figure 2), illustrates that there is instability, i.e., active stress redistribution and elastic failures from unconventional hydrocarbon activities occurring in regions that were otherwise aseismic or quasi-stable. Therefore, the *hazard* potential for a much larger event, in excess

of **M**5.0, is also elevated due to the strain energy influx of multiple microseismic events. As long as the activity causing the instability continues, there are no current means to assess the full *hazard* potential, i.e., the largest potential event, since the subsurface is in a constant non-linear state of stress redistribution flux.

The quantification of *risk* is typically achieved through statistical means, i.e., the likelihood, or probability, of the occurrence of a significant event and its proximity to the structure of interest. Conventional probabilistic seismic hazard analyses (PSHA) require a Poissonian process to determine annual probability of exceedance and is the basis for quantifying acceptable *risk*. This basic statistical model assumes no dependency on past events. However, this is not applicable for assessing the *risk* associated with induced-seismicity. For example, in India, conventional mining activities in the Kolar Gold Fields were generating severe seismic events from rockbursting for almost a century from mining activity. However, once underground mining operations ceased, the seismicity ceased (Krishnamurthy and Shringarputale 1990). Similar examples have occurred in Australia and other intraplate regions, suggesting that the seismic *risk* would be negligible or non-existent should mining operations cease (Ortlepp 2005, Cranswick 2011). The *risk* is amplified in historically aseismic regions where building codes either do not consider or underestimate seismic loading potential or *hazard*. Similarly, the *risk* associated with unconventional hydrocarbon development-induced seismicity is a highly variable quantity that is dependent on activity type, depth, frequency, production levels, regional construction practices, infrastructure conditions, proximity to structures of interest, and past seismicity. Therefore, it cannot be assumed that the *risk* associated with unconventional hydrocarbon development is minimal based solely on past non-occurrence of damage. The associated *risk* changes as industry practices change and expand spatially and temporally, where the redistributed stresses result in a weakened crustal subsurface.

Figures 1, 4, and 6 and Table 4 outline the importance of quantifying the *risk* associated with the unconventional hydrocarbon development-induced seismic hazard. For example, the North Canadian Wastewater Levee and Arcadia Lake Dam have been subjected to nine events between 2011 and 2013, four of which occurred within a three-day timeframe, with a magnitude greater than or equal to **M**4.0, including the 2011 M_w 5.7 Oklahoma event, Figure 1 (Keranen et al. 2013). Furthermore, these events

are epicentrally located within close proximity, in some cases less than 10 km, of federally owned infrastructure (Figures 1 and 6). If current seismic trends continue without fully understanding the *hazard* potential from unconventional hydrocarbon production activities and regions of high induced-seismic density encroach on more federal infrastructure, shown in Figure 6, the *risk* potential can become exponentially compounded.

Figure 6. Study region with federal infrastructure, dams (blue crosses) and levees (red lines), within 30-km buffer zone (purple shaded region) containing at least one known hydraulic fracturing-based unconventional gas production well. Yellow dots are publicly reported epicenters of M2.0 or greater since 2004 within 30 km of at least one known production well. Alphabetic callouts correlate to the largest publicly reported events within 30 km of at least one known production well listed in Table 4.

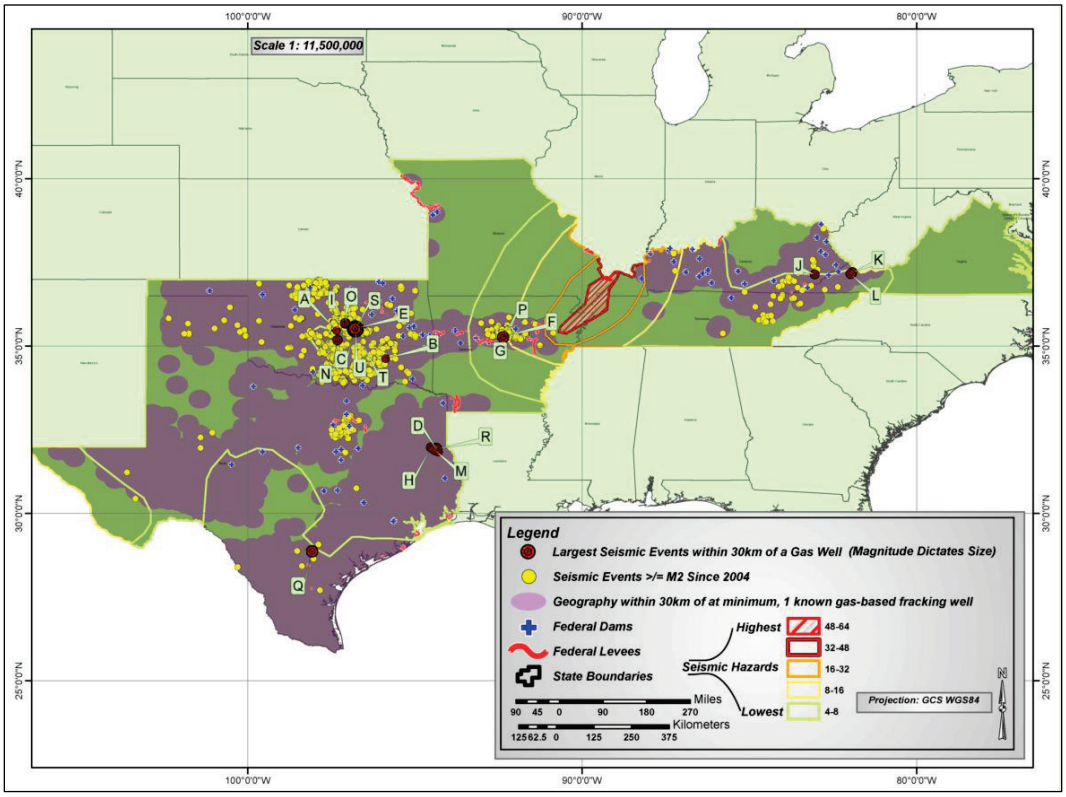

The current maximum-induced *hazard* will vary based on different geological stress regimes. Statistical predictions of maximum potential induced events cannot be justified until the complexity of induced-seismic risk can be adequately bounded, with respect to three critical factors; geology, the unconventional hydrocarbon practices/processes being utilized, and potential failure mechanisms. Furthermore, structures in unconventional hydrocarbon production regions should be continually reassessed as unconventional hydrocarbon development wells are completed throughout a shale basin and observational data are updated. It

must be stressed that this is a simplification of a complex problem and in no way assesses the effects of repetitive seismic straining or non-extreme multiple hazard critical load combinations that may cause structural fatigue or failure.

5 Maximum Induced-Seismicity Potential from Fluid Injection Geo-engineering Activities

The Central United States is experiencing an exponential rise in seismicity in traditionally aseismic regions. The predominant focus of the potential causality has been centered on fluid injection wells, most notably Class II high volume wastewater injection wells and the cumulative effect of multiple injection sites into the same geological lithology. Central to all these studies are two components required to induce earthquakes: (a) a nearby fault or fault system to which slip can occur; and (b) prolonged high fluid injection volumes within a few kilometers of event epicenters. However, significant seismicity is occurring in regions where one or both of these conditions do not exist yet vast extents of unconventional hydro-carbon production (UHP) horizontal hydraulic fracturing wells operate. In this study, we investigate the cumulative seismic potential, based on injected fluid volume, of co-located hydraulic fracturing wells, where the seismic potential of several UHP wells is equivalent to the potential from conventional wastewater injection wells. Further, it is illustrated that this cumulative hydraulic fracturing well effect could explain the seismicity within regions of Arkansas, Oklahoma, and Texas wherein no other regional geo-engineering activity has been reported. Additionally, this study presents a 95% confidence statistical upper bounds to the fluid-induced seismic potential irrespective of the injection purpose, i.e., secondary oil and gas recovery, disposal of waste fluids, geothermal energy, and/or UHP hydraulic fracturing, wherein the seismic potential varies as a power-law function to injected fluid volumes and based on reported UHP injection volumes an event up to M_w6.5 can be expected.

5.1 Overview of fluid injection induced seismicity

Fluid-induced seismicity is a relatively recent phenomenon gaining notoriety after the Rocky Mountain Arsenal induced events in the 1960s (Raleigh et al. 1976; Healy et al. 1968). With the increase in fluid-based geo-engineering activities, technological advances, population growth and worldwide energy consumption increases, there has been an exponential increase in seismic activity throughout regions that are historically aseismic, most notably in the Central United States. Geo-engineering

activities such as reservoir impoundment, mining, wastewater injection, geothermal systems and CO2 capture have been linked directly to induced seismicity (Seeber et al. 2004; Klose 2010; Frohlich et al. 2011; Frohlich 2012; Frohlich and Brunt 2013; Horton 2012; Brodsky and Lajoie 2013; Ellsworth 2013; Gan and Frohlich 2013; Kim 2013; Davies et al. 2013).

Often dismissed is the seismic potential from hydraulic fracturing activities associated with unconventional hydrocarbon production (UHP) as a single hydraulic well typically has the seismic potential of up to a **M**2.0 event. In some regions, e.g., Texas, this magnitude is often too small to be recorded and/or reported as part of the seismic record thus, a single UHP hydraulic fracturing well seismic potential is often dismissed as a non-influence to the current seismicity increase in the Central United States. Prominent seismologists and earthquake engineers have recently issued concern into the seismic potential of UHP hydraulic fracturing activities (Spotts 2014). The process of hydraulic fracturing is essentially equivalent, in terms of induced subsurface stresses, as any to the aforementioned geo-engineering activities linked to significant seismic events, greater than **M**3.0. Further, the genesis of induced seismicity is assumed to occur solely along subsurface fault structures. Contrary to this assumption is that the observed seismicity in the central United States, since 2004, has increasingly occurred in regions where significant fault systems are not known to exist nor has any seismicity been reported until after UHP activities began.

Conditions in intraplate areas are primed to be susceptible to induced earthquakes as the geological stress states are already at critical stress conditions wherein the geological structure is in a quasi-static equilibrium state (Ellsworth 2013; Hough et al. 2003; McGarr 2014). Thus, geo-engineering activities, e.g., deep fluid injection, geothermal injection, and/or UHP wells, that critically affect deep lithologies and alter the existing mechanical state can potentially result in subsurface shear failure, i.e., induced seismicity. However, of most importance for engineering, economic, social and political decision making matrices is the question of what is the largest expected induced seismic event? The results of this research quantify the largest potential induced seismic event in terms of injected fluid volume into the subsurface with a 95% confidence interval. It must be stressed that this quantification does not express the likelihood of occurrence of such event as the data required for a relatively accurate quantification continually evolve, wherein advances in geo-engineering

practices and technologies can significantly alter the induced-seismicity occurrence rates. This manuscript explains the cumulative seismic potential of UHP hydraulic fracturing wells and correlates geo-engineering fluid injection volumes to regional maximum observed seismicity.

5.2 UHP hydraulic fracturing and induced seismicity mechanics

The term "fracing" is commonly, and incorrectly, used to describe all parts of the unconventional hydrocarbon development process. Hydraulic fracturing is the process used to increase the permeability of the geologic formation containing recoverable hydrocarbons and utilizes highly pressurized, low-viscosity fluid containing various chemicals and particulates for fracture development (NRC 2013; Turcotte et al. 2014). The solids in the fluid are called proppant and are forced into the fractures, "propping" them open. This hydraulic fluid mixture is injected into the oil or gas-producing lithology at pressures of approximately 85% of the overburden stress (Turcotte et al. 2014). The hydraulic fracturing process creates a highly permeable zone adjacent to the well casing that allows for the flow of gas back to the surface. In areas where it is allowable, injection wells are also used to stimulate gas flow, for repetitive and multi-stage fracturing and/or disposal of wastewater associated with unconventional hydrocarbon production (NRC 2013; Zou 2013).

The development of the pervasive fractures in the oil or gas lithology from UHP hydraulic fracturing generates micro-failures within the rock mass and small strain energy release. This released compressive (explosive) energy is relatively minor in terms of seismic moment or earthquake magnitude, thus formulating a basis for excluding hydraulic fracturing as a significant potential seismic source. However, this argument overlooks a significant technological aspect of the hydraulic fracturing process: the use of a proppant to maintain open fractures within the rock mass at internal pressures equivalent to the hydraulic fracturing fluid pressure.

As fluid pressures increase to fracture the desired lithology, the forced proppant is pressurized into the void spaces wherein the rock mass is not allowed to behave elastically and relax, i.e., release induced strain energy. Therefore, rock failure in the classical sense cannot occur and only minor seismic energy is observed in the form of fracture re-orientation to a quasi-static equilibrium with the introduction of the proppant. Thus, the induced pressurization from the hydraulic fracturing fluid is entrapped, i.e., does not dissipate within the rock mass even with fluid/gas extraction.

Therefore, unlike deep injection wells, the reduced effective shear strength, τ_r, does not significantly change with time, and additional fluid is not required to maintain elevated equivalent fluid pressures:

$$\tau_r = \left(\sigma' - \Delta u_{hf}\right)\tan\phi' + c \tag{3}$$

where Δu_{hf} is the hydraulic fracturing fluid pressurization; σ' is the effective overburden stress; ϕ' is the internal friction angle of the rock; and c is the internal cohesion of the rock mass. Failure will not occur within the rock mass until the shear stress is reduced such that the driving shear forces, typically gravitational forces, exceed that of the internal rock (or fault) strength. In cases where no natural boundary condition exits, e.g., faults or geological discontinuities, the competent rock mass surrounding a hydraulically fractured zone will support the excess gravitational stresses not carried by the reduced shear strength zone, akin to bridge spans. As the zones of reduced shear capacity increase, the stresses will no longer be carried by the reduced volume of competent rock resulting in shear (slip) failure. There is no seismological and geological means to differentiate between internal failure of rock along natural bedding fracture planes, geological discontinuities and natural faults, which readily explains the "discovery" of new faults, especially in regions where there has been no sign of seismic activity prior to geo-engineering efforts. Moment tensors, energy release, and wave traces would all be identical in form and function as the release or failure mechanisms are identical, i.e., slip between two solids bonded by frictional forces (McGarr et al. 2009). Typically, the hydraulic fracturing pressures are 85% of the effective overburden stress, resulting in a reduced shear capacity of only 15% of the pre-fractured rock mass strength. With the use of a proppant, this reduction in strength is relatively permanent. In aseismic regions, where the lithology is at a quasi-stable static equilibrium, such a permanent massive reduction in shear strength can cause shear failures along internal fissures, faults, or discontinuities that would otherwise not be susceptible to failure.

This is mechanically no different than modeling hydraulic reduced friction with elevated pore pressure failures as equivalent to a deep fluid injection well in highly permeable lithology. The only significant difference in failure mechanics is that in highly permeable lithology, the pore fluid pressures migrate hydraulically and fluid injection need only occur in a few locations with continual injection to maintain elevated hydraulic pressures over a small topographic region, hereafter referred to a seismic

patch [SP]. For UHP hydraulic fracturing lithologies, the permeability is several orders of magnitude lower (Zou 2013; Gale et al. 2007), thus the fluid and pressures do not migrate throughout the rock (shale) formation. There is no requirement for continual fluid due to the use of a proppant. Therefore, multiple UHP hydraulic fracturing wells are required to replicate pore fluid dispersion effects as modeled for deep injection wells. This is the case in current UHP industry practice and mechanically explains why a single UHP hydraulic fracturing well does not typically pose a significant seismic threat, except in rare cases of high-pressure, high-volume hydraulic fracturing wells, and is the basis of excluding UHP hydraulic fracturing wells as a potential seismic sources. However, it is the close spatial density of multiple UHP hydraulic fracturing wells, or well systems (defined as a series of adjacent UHP hydraulic fracturing wells covering 2.8 km^2 area), operating over a 78 km^2 topographic SP and at the same lithology depth that presents a seismic hazard equivalent to deep injection wells.

5.3 Correlations between all fluid injection processes and induced seismicity

McGarr (2014) presents a straightforward relationship for determining maximum induced seismic magnitude from a number of case studies that deal with fluid injection into the subsurface for different applications, i.e., wastewater disposal, enhanced geothermal, hydraulic fracturing, and injection for scientific studies. His inclusion of case histories covers different global locations, geologic settings, and injection applications that formulate the basis for his maximum seismic potential upper boundary line. Figure 1 illustrates that it is the volume of the injected fluid, not the purpose of the well, that influences the seismic potential. The relatively straightforward relationship (McGarr 2014) is valid only under a series of significant assumptions: (1) all the injected fluid is seismogenic; (2) that the highly permeable layer is fully saturated; (3) that elastic and mechanical properties of the injecting lithology can be generalized by a single shear modulus; (4) that the injection lithology is at exactly half a seismic stress drop from failure; and (5) the fluid intersects a nearby fault or fault system. However, some of the assumptions made in generating this upper boundary relationship contain large uncertainties and broad assumptions, over-simplifications of rock mechanics, geological lithologies, injection fluid response in respect to time and dispersion, and/or seismic activity rates.

McGarr (2014) derives an "upper bound" relation for the Maximum Magnitude for induced events (from fluid injection) using the equation:

$$\Sigma M_0 = \frac{2\mu(3\lambda + 2G)}{3} \cdot \Delta V \tag{4}$$

$$M_0(max) = G\Delta V \tag{5}$$

where McGarr (2014) defines G as the modulus of rigidity, constant at 3.0×10^{10} Pa, and ΔV is the injected fluid volume. However, research on mechanical and elastic properties of shales, including the Barnett shale, illustrates a wide range of values from 4.5 to 61 GPa and 0.03 to 0.3 for Young's modulus, E, and Poisson's ratio, ν, respectively (Gale et al. 2007). From these values the maximum potential seismic moment, using McGarr's (2014) derivation, can exceed double that of Eq 5 for the same injected fluid volume. If McGarr's (2014) assumption that the entire SP region is exactly half a stress drop from failure is applied, then the seismic potential from Gale et al. (2007) and that of McGarr (2014) are similar. However, there is no basis for all SP regions being exactly half a stress drop from failure except to simplify the mathematics.

However, McGarr's (2014) G parameter is not physically the shear modulus (or modulus of rigidity), rather it is the shear rupture strength of the seismogenic SP source due to the frictional coefficient, μ, wherein a mean laboratory value of 0.6 is assumed and explains why the geological rock mechanics properties (Gale et al. 2007) yield a lower, one order of magnitude or more, shear modulus than the 3.0×10^{10} Pa assumed by McGarr (2014). Additionally, McGarr's "upper bound" limit is identical to standard equation of seismic moment for elastic rebound theory:

$$M_o(max) = G\Delta V = \mu_k A\bar{D} \tag{6}$$

where μ_k is the fault rupture strength; A is the slip area; and $\bar{D}$ is the average slip. However, the failure mechanics are not the same between elastic rebound theory and induced seismicity. This difference is further evidenced by the mean trend of McGarr's (2014) maximum seismic event data wherein the data mean intersects the McGarr (2014) seismic limit, as in Figure 7. Thus, Equation 5 does not follow the observational data for induced seismicity as it intersects the mean event data trend line, so an intersection of a proposed "upper boundary" line with mean trend data results in no statistical meaning of the proposed boundary, in terms of confidence and/or accuracy.

Figure 7. Comparison of McGarr (2014) upper seismic limit equation and derived power-law mean, blue line, and 95% confidence upper bound, black dashed line, Mo(max) predictive equations. All case studies shown in this figure are from McGarr (2014).

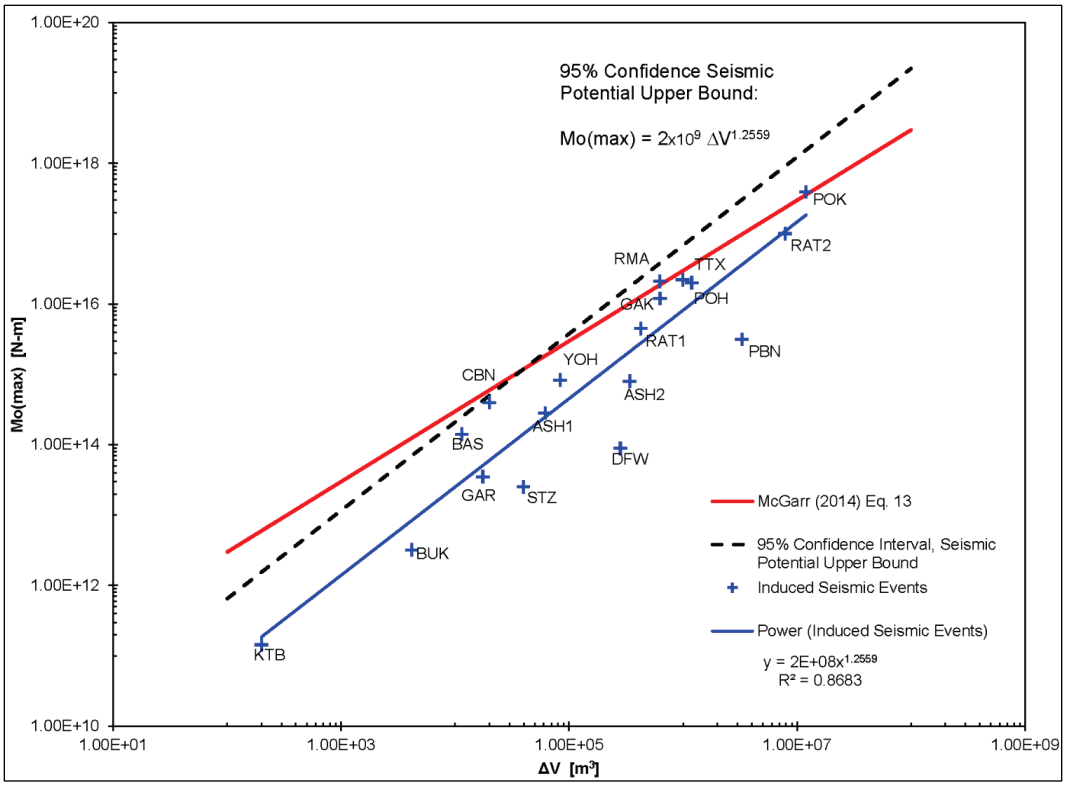

Figure 7 shows that there is a strong power-law correlation, $R^2 = 0.87$, between the total volume of injected fluid and the largest observed maximum seismic moment:

$$M_o(max) = 2x10^8\ \Delta V^{1.225} \tag{7}$$

Equation 7 illustrates the mean observational maximum induced seismic moment associated with the injection of fluids into the subsurface, irrespective of injection purpose. Furthermore, a power-law relationship more accurately describes processes, phenomena, and hazards associated with natural processes or components, e.g., floods, hurricanes, earthquakes, and earthquake engineering.

Assuming a normal distribution about the mean data trend and applying 2σ, where σ is the standard deviation of McGarr's (2014) dataset, a statistical upper boundary with a 95% confidence interval can be approximated as:

$$M_o(95\%CI) = \left(2x10^8 + 2\sigma\right)\Delta V^{1.225} \simeq 2x10^9\,\Delta V^{1.225} \quad (8)$$

The seismic moment can be expressed in terms of moment magnitude, M_w, as (McGarr 2014):

$$M_w = \frac{\log M_o - 9.05}{1.5} \quad (9)$$

Additionally, the seismic potential from a single UHP hydraulic fracturing well can be quantified in the form of the total potential strain energy, U_e, stored within the rock mass over a given domain, V:

$$U_e = \iiint_V U dx dy dz \quad (10)$$

During the hydraulic fracturing process the rock mass is fractured and deforms proportionally with the quantity of injected fluid volume. The deformations are effectively permanent due to the proppant; thus, on a first order analysis it can be assumed that the net work done on the rock mass is equal to the stored potential strain energy. Assuming that the strain energy is caused by uniform shear stress from hydraulic fluid injection, the imparted strain energy can be determined:

$$dU = \frac{1}{2}\tau_{xy}\left(\frac{\partial u}{\partial y} + \frac{\partial v}{\partial x}\right)dx dy dz \quad (11)$$

From Equation 11, the total potential strain energy density, in terms of shear modulus, G, and shear strain, γ_{xy}, can be approximated:

$$U = \frac{G}{2}\gamma_{xy}^2 \quad (12)$$

Combining Equations 10 and 12 with an average hydraulic fluid volume (15,000 m^3), typical horizontal drill length (1 km), a radial fracture extent (10 m), and a typical shear modulus (23.5 GPa), the total stored potential strain energy is approximately 1.76 x 10^{13} N-m. Assuming that all the strain energy is released during a single slip failure, the resulting event would be to the order of M_w2.8. This result is in relative agreement with a mean estimate of the maximum seismic potential, Equation 5, of **M**3.0. It

must be stressed that estimating the seismic potential from Equations 10 through 12 is an isotropic estimation and does not account for geological variability, anisotropy, nor any naturally stored potential strain energy within the rock mass, and, therefore, the authors recommend Equations 5 and 6 be used.

The uncertainties noted in geological formations, hydrological models, and mathematical derivations (McGarr 2014; Keranen et al. 2013; 2014) are implicitly accounted for within the determination of the dataset mean and in Equations 7 and 8. Moreover, Equations 7 and 8 implicitly account for variable initial geological and hydrological conditions, represented mathematically in the power-law coefficient and are not subjected to the same assumptions as McGarr (2014). Equation 6 encompasses 100% of McGarr's (2014) data; whereas the upper limit set by McGarr (2014), Equation 5, encompasses only 88.8% of the same dataset.

5.4 Correlations between UHP hydraulic fracturing fluid injection and induced seismicity observations

To investigate the seismic potential of UHP hydraulic fracturing fluid injection (Equation 8) with observed seismicity, a GIS-based approach was developed incorporating natural gas development information, seismic events, fault locations, and deep injection well locations.

A complete detailed account of the GIS framework, methodology, and analysis can be found in the third technical report of this series ("Unconventional Hydrocarbon Development Induced Seismic Hazards Within the Central United States: Report 3, Analytical GIS Methodology").

Due to proprietary regulations, this research defines a UHP well system as a 2.8 km^2 surface area that contains, at minimum, one hydraulic fracturing well (Figure 8) whose location and fluid injection volume in conjunction with deep injection well locations are derived from publicly available sources, e.g., U.S. Geologic Survey, FracFocus.org, state regulatory agencies, etc. (USEIA 2011; USGS 2008; USGS 2012; FracFocus.org 2014; AOGC 2011; ArcGIS 2013; TRRC 2014; Skytruth 2013; OCC 2013). Seismic events for the three states use state, regional, and national sources to make a composite catalog; the main focus is on events from 2004 to 2013 of M3 or greater (AGS 2013; OGS 2013; CERI 2013; ANSS 2013; NEIC 2013). Fault maps for the areas are from state and national databases (USGS 2005; 2013).

Figure 8. Location of 15 random seismic patches (SP) along with seismic events with M3 or greater from 2004 to 2013, UHP well systems, basin and play locations (USEIA 2011) in Arkansas, Oklahoma, and Texas. Yellow call-out illustrates the UHP well system coverage within a 78 km2 SP. The orange call-out illustrates the individual UHP well borings within a single well system and locations of reported deep injection wells.

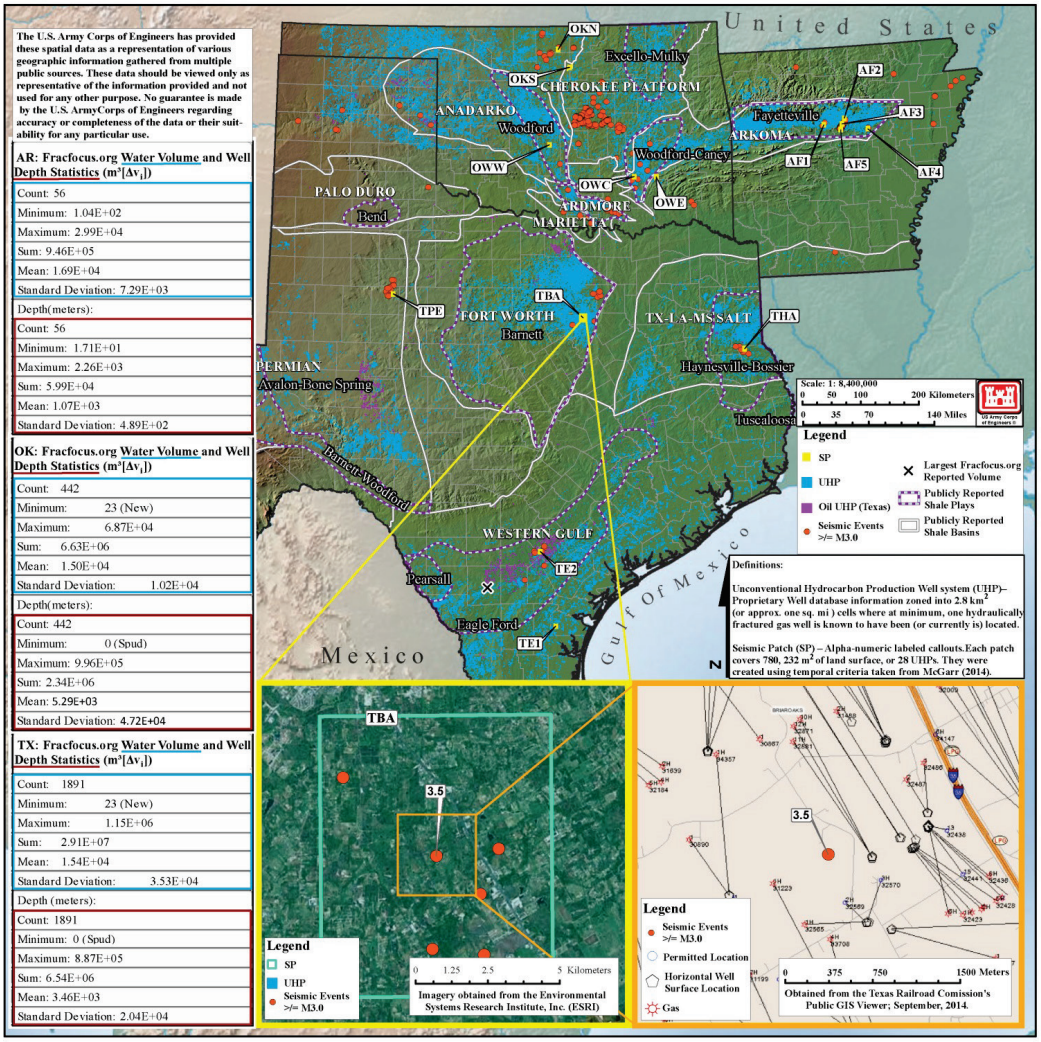

A complete detailed account of the seismic catalog can be found in the second technical report of this series ("Unconventional Hydrocarbon Development Induced Seismic Hazards Within the Central United States: Report 2, Seismic Catalog").

Figure 8 illustrates that each of these UHP well systems can contain in excess of 20 individual wells (TRRC 2014). However, in terms of injected UHP fluid volume, it is assumed that a single UHP well system's geological formation is subjected to the average publicly reported fluid injection of a single UHP well within that SP region. Therefore, irrespective of the number of individual well pads and horizontal borings within a UHP well

system, the elevated equivalent fluid pressure (Equations 3, 7, and 8) cannot exceed the injected hydraulic fluid volume of an individual well. It must be noted that this research uses an average value to be conservative knowing that not all 2.8 km^2 of a SP is subjected to hydraulic fracturing pressures. The actual injected volumes in any region may be elevated. This limitation is required to account for the low hydraulic conductivity of the shale formations where fluid dispersion only occurs within the immediate vicinity of the fracture growth extents.

McGarr (2014) and Keranan et al. (2013; 2014) used the cumulative influence of multiple high-volume deep injection wells for the total injected fluid input requirement to account for the observed seismic moment release for the 2011 M_w5.7 Prague, OK, earthquake. Therefore, for consistency and SP regional limitations, the maximum SP over which the summation of seismic influence from UHP well systems can be calculated is the same 78 km^2 landmass; a maximum of 28 UHP well systems.

Fifteen random regions were selected, five in each major UHP state (Arkansas, Oklahoma, and Texas), wherein a **M**3.0+ seismic event has been observed since 2004. In each 78 km^2 SP region selected, the number of well systems, average hydraulic fracturing fluid volume, proximity to known faults, and location of reported deep injection wells were calculated (Figure 8 and Table 5.) In 40% of the selected regions there were no known fault systems, and 60% did not report the presence of deep injection wells. Additionally, two theoretical SP regions, 9CI and OMV, are included in Table 5 to illustrate the limit potential of Equation 8. The 95% confidence seismic limit potential, 9CI, is calculated as the maximum of the mean plus 2σ reported hydraulic fracturing fluid volume applied to a fully covered SP region. An example would be Texas, with a 95% fluid volume confidence level of 8.58×10^4 m^3 per UHP system for a total volume of 2.56×10^6 m^3 and M_w5.5 event, Equations 8 and 9. The maximum seismic potential based on the largest single well reported hydraulic fracturing fluid volume, OMV, is from the Eagle Ford (Texas) shale at 1.15×10^6 m^3. Assuming this reported volume is applied to a fully covered SP region, the maximum induced seismic event is M_w6.5, as in Equations 8 and 9.

Table 5. Tabulated data for 15 randomly selected SP within the study region.

Name	Shale Play or Basin	UHP Area (km^2)[1]	Max Obs. Seismic Event in SP[6]	Shortest Distance[3] to Known Fault (km)	Inject. Well[5]	Inject. Well[7] Proximity (km)	Avg. Single Well Water Volume [m^3] (Δv_i)	ΔV Total SP Fluid Volume [m^3] ($\sum \Delta vi$)	Mean M_{max} (Eqn. 5)	*95% Confidence Bound M_{max} (Eqn. 6)*
AF1	Fayetteville	65.5	3.4	0	N	7.8	2.26E+04	5.08E+05	4.3	4.9
AF2	Fayetteville	78.0	3.3	0	N	3.1	1.69E+04	4.48E+05	4.2	4.9
AF3	Fayetteville	61.8	4.7	0	Y (1)	0.0	1.69E+04	4.74E+05	4.3	4.9
AF4	Fayetteville	53.4	3.3	0	N	7.0	1.69E+04	3.17E+05	4.1	4.8
AF5	Fayetteville	13.4	3.9	0	Y (1)	0.0	2.16E+04	8.84E+04	3.6	4.3
OKS	Cherokee Platform	31.1	3.7	0	Y (1)	0.0	1.50E+04	1.04E+05	3.7	4.4
OKN	Cherokee Platform	19	3.5	1.5 S	Y (6)	0.0	1.50E+04	5.19E+04	3.4	4.1
OWC	Woodford	69	3.2	0	N	1.6	1.50E+04	3.29E+05	4.1	4.8
OWW	Woodford	73.6	3.4	0.3 N	N	3.8	2.61E+04	1.16E+05	3.7	4.4
OWE	Woodford	13.4	4.0	0	N	19.2	1.50E+04	6.92E+04	3.6	4.2
TE1	Eagle Ford	69.4	3.9	62 NW	Y(1)	0.0	1.53E+04	2.12E+05	4.0	4.6
THA	Haynesville	17.9	4.8	0	N	1.2	1.53E+04	4.42E+04	3.4	4.1
TPE	Permian Basin	16.1	4.3	141 NE	N	2.2	1.53E+04	3.83E+04	3.3	4.0
TBA	Barnett	78	3.5	40.5 NW	N	0.3	1.61E+04	2.11E+05	4.0	4.6
TE2	Eagle Ford	39.3	4.8	1.6 NW	Y(1)	0.0	2.50E+04	4.32E+05	4.2	4.9
9CI[2]	NA	78	NA	NA	NA	NA	8.58E+04	2.56E+06	4.9	5.5
OMV[4]	Eagle Ford	78	NA	NA	NA	NA	1.15E+06	3.44E+07	5.8	6.5

Notes

1. A UHP (Unconventional Hydrocarbon Production) Well System is defined as having at least one well in a 2.8 km^2 area.
2. 2. 9CI = 95% Confidence Interval boundary for UHP well systems, wherein the fluid volume is two standard deviations above the mean for any region. This is a theoretical situation and not reflective of an observed scenario.
3. If distance to fault system is zero then there is a known fault system in seismic patch.
4. OMV = Observed Maximum Volume. This scenario uses real observed volume and assumes that all UHP well systems are using that volume.
5. Injection Well information is thru 2013 for the Seismic Patch in order to compliment the time interval of the observed seismicity. The number of Injection wells within the SP is given in parentheses.
6. SP is for Seismic Patch.
7. Injection Well proximity is the closest distance between an injection well and the seismic patch if there is not a well within the seismic patch; value is zero if there is a well present in seismic patch.

The 15 random SP regions are included in addition to McGarr's (2014) dataset, Figure 9, to illustrate the accuracy of Equation 8, wherein 97.0% of the observed data is encompassed by the 95% confidence upper bound. Only THA falls outside the predicted limit; however, closer examination of

this SP region indicates the presence of numerous hydraulic fracturing oil wells operating at the same geological depths as UHP hydraulic fracturing wells. These oil wells were not included in the original analysis focusing on only natural gas activities, Table 5, but readily explain the under-prediction of Equation 8. If the total oil well hydraulic fracturing fluid is included, then the upper limit prediction, Equation 8, is equivalent to the observed seismic event. Conversely, Equation 5 has a predictive accuracy of 84.8% with noted over-predictions for low fluid volume activity and is under-predictive for large fluid volumes, as in Figure 7.

Figure 9. Proposed seismic potential upper boundary, at a 95% confidence, from Equation 6. Blue data points are from McGarr (2014) case studies and red data points are the cumulative seismic potential from 15 randomly selected seismic patches, shown in Table 5.

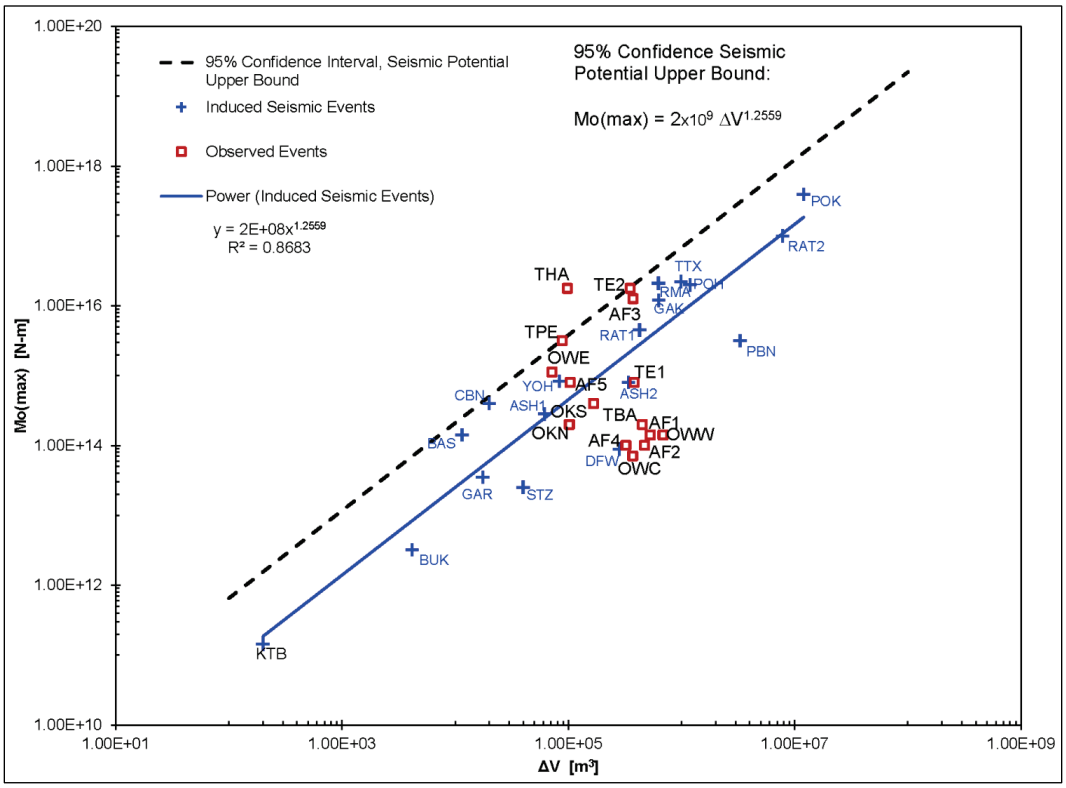

Based on reported fluid injection numbers for UHP hydraulic fracturing wells, the mean fluid volume for all states -- Arkansas, Oklahoma, and Texas -- is 15,342 m^3 per well. Thus, the maximum seismic potential from an average well is 2.9×10^{13} N-m or M_w3 event, shown in Equations 8 and 9. This is at the lower threshold limit of instrument sensitivity in Texas and, as such, most of these events would be neither reported nor detected. However, this upper limit, based on an average hydraulic fluid volume for a single well, is in good agreement with observed single well hydraulic

fracturing induced events within the study region, e.g., Garvin County, Oklahoma (McGarr 2014; Holland 2013), and worldwide, e.g., Bowland Shale, UK (McGarr 2014; De Pater and Baisch 2011).

5.5 Hazard prediction conclusions

Based on various fluid injection geo-engineering activities (wastewater, geothermal, hydraulic fracturing), a power-law correlation between induced seismic moment and total injected fluid volume was observed for worldwide known seismic causalities. A statistical 95% confidence upper boundary was applied to the original dataset wherein all observational data points fit below the upper threshold (Equation 8) an accuracy improvement over previous research of 88.8% (McGarr 2014). Unlike previous research, the proposed power-law relationship implicitly accounts for variability and uncertainties in initial subsurface stress states, saturation, elastic and mechanical properties, and failure mechanisms irrespective of fluid injection purpose. Figure 7 illustrates that the observed seismicity for the largest injection case study, the 2011 $M_w5.7$ Prague, OK, event, is actually close to the mean value of anticipated induced seismicity (Equation 7) for that volume of injected fluid, $M_w5.4$, and not an "upper" limit as predicted by McGarr (2014). The 95% upper boundary (Equation 8) for the same injection volume indicates a maximum event, $M_w6.1$, should be the expected hazard.

To understand the seismic potential from single UHP hydraulic fracturing wells, Equation 8 is applied to known UHP fluid injection volumes. From McGarr's (2014) published hydraulic fracturing fluid data correlated to induced seismic events (Figure 7 and Equation 8), a single UHP hydraulic fracturing well can induce up to a $M_w3.6$ event. Based on highest single UHP hydraulic fracturing well publicly reported fluid volumes, $1.15x10^6$ m^3, this upper seismic potential increases to $M_w5.1$ for a single well.

To understand the effects of multiple UHP hydraulic fracturing wells within a general landmass, a GIS approach was incorporated using the same landmass area, referred to as a seismic patch, that was used by other researchers for summation of Class II deep injection wells, 78 km^2 (McGarr 2014). Due to the lack of hydraulic conductivity within shale lithology, each seismic patch was divided into 2.8 km^2 cells, wherein each cell could only effectively "inject" a fluid volume equal to the mean for a single UHP well in that region, irrespective of the number of physical wells operating within the cell. Therefore, the cumulative effect of multiple 2.8 km^2 UHP hydraulic

fracturing well systems operating with a seismic patch can be calculated in terms of total well system fluid volumes. Fifteen randomly selected 78 km^2 seismic patches were selected and compared to proposed 95% confidence upper bound seismic limit (Equation 8). Figure 9 illustrates a 97% accuracy of Equation 8 and that the cumulative effect of multiple UHP hydraulic fracturing well systems within the same seismic region has the same seismic potential as high-volume injection wells. Applying the cumulative potential to the largest known UHP hydraulic fracturing volumes, Eagle Ford shale in Texas, the maximum seismic potential from UHP hydraulic fracturing activities can reach an $M_w6.5$ event.

The findings of this research present an updated means for estimating the seismic potential for all geo-engineering activities, not just UHP hydraulic fracturing. It must be stressed that the authors acknowledge the breadth of research completed in correlating deep injection well activities with induced seismicity, and it is not the intention to replicate these findings. The focus on UHP hydraulic fracturing is not meant to portray hydraulic fracturing as the sole causality in the increase of seismicity within the Central United States, but rather as an additional contributor to the seismic increase.

Of particular importance to the community at large is a means to mitigate the induced seismic hazard. Based on the findings presented herein, a first order mitigation strategy could be to limit the future activity in any one region in terms of both allowable fluid injection volume and geo-engineering density. Limitations in one or both of these parameters would reduce the seismic potential from Equation 8. However, this first order mitigation strategy does not reduce the hazard potential for regions with current geo-engineering activity, specifically UHP wells where time-dependency injection rates are not applicable. Further, the effects of well abandonment and subsurface subsidence are not considered but are the subject of future research efforts.

5.6 Hazard prediction limitations

There are inherent errors in magnitude, depth, locations, and origins in publicly available earthquake catalogs, which are continually updated. Well information from all database sources has been randomly cross-checked with no data discrepancies between catalogs identified; therefore, the publicly reported information is considered valid with the understanding that well information and water volume numbers can vary in quality or

often go unreported. This paper does not model hydrological subsurface conditions from injected water. Construction of the seismic patches (surface area of 78 km^2) does not account for spherical divergence or influence from other engineering activities outside of the patch or other subsurface conditions, e.g., faults or fractures within close proximity to a patch boundary. As such, the quantified magnitudes presented herein may vary for specific locations, wherein a specific region of interest could exceed presented values. However, this uncertainty would not affect the confidence boundary prediction, Equation 8, but rather the magnitude of the total injected volume used to determine the maximum potential event.

References

Advanced National Seismic System (ANSS). 2013. Advanced national seismic system earthquake catalog. http://www.ncedc.org/anss/catalog-search.html.

ArcGIS. 2013. Hydraulically-fractured gas and injection well locations in Oklahoma, ArcGIS Online. http://www.arcgis.com/home/item.html?id=aa7f85ff6fb149248df33ba2aae66080.

Arkansas Geological Survey (AGS). 2013. Arkansas Geological Survey catalog. http://www.geology.ar.gov/geohazards/earthquakes.htm.

Arkansas Oil and Gas Commission (AOGC). 2011. The Arkansas oil and gas commission, general rule H-1 fault map. http://www.aogc.state.ar.us/images/General%20Rule%20H-1%20Fault%20Map.pdf.

Båth, M. 1984. Rockburst seismology. In Proceedings, *1st International Symposium on Rockbursts and Seismic Activity in Mines*, 1982, 7-15. Johannesburg, Republic of South Africa.

Baxter, C. D., P. J. Trautman, and O.-D. S. Taylor. 2013. *Volumetric change of silts following cyclic loading*. URITC PROJECT, University of Rhode Island Transportation Center Final Report. Kingston, RI: University of Rhode Island.

Bennett, T. J., and K. L. McLaughlin. 1997. Seismic characteristics and mechanisms of rockbursts for use in seismic discrimination. In *Proceedings, 4th International Symposium on Rockbursts and Seismic Activity in Mines, 11-14 August 1997,* ed. S. J. Gibowicz and S. Lasocki, 61-66. Krakow, Poland.

Bolstad, D. D. 1990. *Rockburst control research by the U.S. Bureau of Mines. In Proceedings, Keynote Lecture: 2nd International Symposium on Rockbursts and Seismic Activity in Mines, 8-10 June 1988*, ed. C. Fairhurst, 371-375. Minneapolis, MN: University of Minnesota.

Bradshaw, A. S., H. Miller, and C. D. P. Baxter. 2007. *Monitoring ground movements of a braced cut in providence silt*. 7th International Symposium on Field Measurements in Geomechanics. Boston, MA.

Brodsky, E., and L. Lajoie. 2013. Anthropogenic seismicity rates and operational parameters at the Salton Sea Geothermal Field. *Science* 341(6145):543-546.

Burchett, R. R., K. V. Luza, O. J. Van Eck, and F. W. Wilson. 1985. *Seismicity and tectonic relationships of the Nemaha uplift and midcontinent geophysical anomaly*. Final project summary, Oklahoma Geological Survey, Special Publication Norman, OK: University of Oklahoma.

Center for Earthquake Research Information (CERI). 2013. New Madrid catalog. http://folkworm.ceri.memphis.edu/catalogs/html/cat_nm.html.

Cook, N. G. W. 1964. The application of seismic techniques to problems in rock mechanics. *International Journal of Rock Mechanics and Mining Sciences* 1:169-179.

Cook, N. G .W. 1976. Seismicity associated with mining/induced seismicity. *Engineering Geology* 10(2-4):99-122.

Chamber of Mines Research Organization (CMRO). 1988. *An industry guide to methods of ameliorating the hazards of rockfalls and rockbursts*. 1988 Edition. Johannesburg: Chamber of Mines of South Africa.

Cranswick, E. 2011. *Coincidence of mines and earthquakes in Australia*. Australian Earthquake Engineering Society 2011 Conference. Barossa Valley, South Australia.

Curtis, J. B. 2002. Fractured shale-gas systems. *American Association of Petroleum Geologists* 86(11):1921-1938.

Davies, R., G. Foulger, A. Bindley, and P. Styles. 2013. Induced seismicity and hydraulic fracturing for the recovery of hydrocarbons. *Marine and Petroleum Geology* 45:171-185.

Davis, K. 2004. J. Goff's pub on point street was condemned and is considered to be a safety hazard. In *Providence Journal*. Providence, RI: GateHouse Media.

De Pater, C. J., and S. Baisch. 2011. *Geomechanical study of Bowland Shale seismicity*. Lichfield, UK: Cuadrilla Resources Ltd.

Dunlop, R., and S. Gaete. 1997. Controlling induced seismicity at El Teniente Mine: The Sub-6 case history. In *Proceedings, 4th International Symposium on Rockbursts and Seismic Activity in Mines, 11-14 August 1997,* ed. S. J. Gibowicz and S. Lasocki, 233-236. Krakow, Poland.

Ellsworth, W. L. 2013. Injection-Induced Earthquakes. *Science* 341(6142):1225942.

FracFocus. 2014. http://fracfocus.org/.

Frohlich, C. 2014. Induced or triggered earthquakes in Texas: Assessment of current knowledge and suggestions for future research. http://earthquake.usgs.gov/research/external/reports/G12AP20001.pdf.

Frohlich, C., C. Hayward, B. Stump, and E. Porter. 2011 The Dallas-Fort Worth earthquake sequence; October 2008 through May 2009. *Bulletin of the Seismological Society of America* 101:327-340.

Frohlich, C. 2012. Two-year survey comparing earthquake activity and injection-well locations in the Barnett Shale, Texas. *Earth, Planetary and Atmospheric Sciences. Proceedings of National Academy of Science* 109(35):13934-13938.

Frohlich, C., and M. Brunt. 2013. Two-year survey of earthquakes and injection/production wells in the Eagle Ford Shale, Texas, prior to the MW4.8 20 October 2011 earthquake. *Earth and Planetary Science Letters* 379:56-63.

Frohlich, C., and S. Davis. 2002. Texas earthquakes. Austin: University of Texas Press.

Gale, J., R. Reed, and J. Holder. 2007. Natural fractures in the Barnett Shale and their importance for hydraulic fracture treatments. *AAPG Bulletin* 91(4):603–622.

Gan, W., and C. Frohlich. 2013. Gas injection may have triggered earthquakes in the Codgell oil field, Texas. *Proceeding of National Academy of Sciences* 110(47):18786-18791.

Gay, S. P. 2003. The Nemaha trend – A system of compressional thrust-fold, strike-slip structural features in Kansas and Oklahoma, part 2. *Shale Shaker* 54:39-49.

Gay, N. C., and W. D. Ortlepp. 1978. Anatomy of a mining-induced fault zone. *Geological Society of America Bulletin* 90(1):47-58.

Gibowicz, S. J., and A. Kijko. 1994. *An introduction to mining seismology*. New York: Academic Press.

Gutenberg, B. 1945a. Amplitudes of surface waves and magnitudes of shallow earthquakes. *Bulletin of the Seismological Society of America* 35:3-12.

_____. 1945b. Amplitudes of P, PP, and S and magnitude of shallow earthquakes. *Bulletin of the Seismological Society of America* 35:57-69.

Gutenberg, B., and C. F. Richter. 1944. Frequency of earthquakes in California. *Bulletin of the Seismological Society of America* 34(4):163-191.

Gutenberg, B., and C. F. Richter. 1949. *Seismicity of the earth and associated phenomena*. Princeton, NJ: Princeton University Press.

Healy, J. H., W. W. Rubey, D. T. Griggs, and C. B. Raleigh. 1968. The Denver earthquakes. *Science* 161(3848):1301–1310.

Holland, A. 2013. Earthquakes triggered by hydraulic fracturing in south-central Oklahoma. *Bulletin of the Seismological Society of America* 103(3):1784–1792.

Homeland Security Infrastructure Program (HSIP). 2012. Homeland Security (HLS) and National Preparedness – Prevention, protection, mitigation, response and recovery (NP-PPMR&R) Communities; NGA Case 12-424. Washington, DC: Department of Homeland Security.

Horton, S. 2012. Disposal of hydrofracking waste fluid by injection into subsurface aquifers triggers earthquake swarm in central Arkansas with potential for damaging earthquake. *Seismological Research Letters* 83(2):250-260.

Hough, S. E., L. Seeber, and J. G. Armbruster. 2003. Intraplate triggered earthquakes: Observations and interpretations. *Bulletin of the Seismological Society of America* 93(5):2212–2221.

Idriss, I. M. 1985. Evaluating seismic risk in engineering practice. In *Proceedings of the 11th International Conference on Soil Mechanics and Foundation Engineering, 12-16 August 1985*, 1:255-320. San Francisco, CA.

Kaneko, K., K. Sugwara, and Y. Obara. 1990. Rock stress and microseismicity in a coal burst district. In *Proceedings, 2nd International Symposium on Rockbursts and Seismic Activity in Mines, 8-10 June 1988,* ed. C. Fairhurst, 183-188. Minneapolis, MN: University of Minnesota.

Keranen, K. M., H. M. Savage, G. A. Abers, and E. S. Cochran. 2013. Potentially induced earthquakes in Oklahoma, USA: Links between wastewater injection and the 2011 Mw 5.7 earthquake sequence. *Geology* 41(6):699-702.

Keranen, K., M. Weingarten, G. Abers, B. Bekins, and S. Ge. 2014. Sharp increase in central Oklahoma seismicity since 2008 induced by massive wastewater injection. *Science* 345(6195):448-451.

Kim, W.-Y. 2013. Induced seismicity associated with fluid injection into a deep well in Youngstown, Ohio. *Journal of Geophysical Research: Solid Earth* 118(7):3506-3518.

Kisslinger, C. 1976. A review of theories of mechanisms of induced seismicity. *Engineering Geology* 10(2-4):85-98.

Klose, C. D. 2010. Human-triggered earthquakes and their impacts on human security, achieving environmental security: Ecosystem services and human welfare. In *NATO science for peace and security series - E: human and societal dynamics.* ed. P.H. Liotta et al., 69:13-19. Amsterdam: IOS Press.

Kramer, S. L. 1996. *Geotechnical earthquake engineering*. Upper Saddle River, NJ: Prentice-Hall Inc.

Krishnamurthy, R., and S. B. Shringarputale. 1990. Rockburst hazards in Kolar gold fields. In *Proceedings, 2nd International Symposium on Rockbursts and Seismic Activity in Mines, 8-10 June 1988,* ed. C. Fairhurst, 411-419. Minneapolis, MN: University of Minnesota.

Lenhardt, W. A. 1988. Some observations regarding the influence of geology on mining induced seismicity at Western Deep Levels Limited. In *Proceedings of 2nd Regional Conference for Africa, SANGORM*, 45-48. Swalizand.

Lenhardt, W. A. 1990. Damage studies at a deep level African gold mine. In *Proceedings, 2nd International Symposium on Rockbursts and Seismic Activity in Mines, 8-10 June 1988,* ed. C. Fairhurst, 391-393. Minneapolis, MN: University of Minnesota.

Lenhardt, W. A. 1992. Seismicity associated with deep level mining. *Acta Montana, Series A* 2(88):179-192.

Li, S. L., and R. Guo. 2001. Development of rockburst research for metal mines in China. In *Proceedings, 5th International Symposium on Rockbursts and Seismic Activity in Mines, 17-19 September 2001,* 225-228. Johannesburg, Republic of South Africa.

Llenos, A., and A. Michael. 2013. Modeling earthquake rate changes in Oklahoma and Arkansas: Possible signatures of induced seismicity. *Bulletin of the Seismological Society of America* 103(5):2850-2861.

Martin, R. J. 1972. Time-dependent crack growth in quartz and its application to the creep of rocks. *Journal of Geophysical Research* 77(8):1406-1419.

Maury, V. M. R., J.-R. Grasso, and G. Wittlinger. 1976. Monitoring of subsidence and induced seismicity in the Lacq gas field (France): The consequences on gas production and field operation. *Engineering Geology* 32:123-135.

McClain, W. C. 1970. *On earthquakes produced by underground fluid injection*. ORNL-TM-3154. Oak Ridge, TN: Oak Ridge National Laboratory.

McGarr, A. 1971. Violent deformation of rock near deep-level tabular excavations-seismic events. *Bulletin of the Seismological Society of America* 61(5):1453-1466.

McGarr, A. 1984. Some applications of seismic source mechanism studies to assessing underground hazards. In *Proceedings, 1st International Symposium on Rockbursts and Seismic Activity in Mines, 1982,* 199-208. Johannesburg, Republic of South Africa.

McGarr, A., M. Boettcher, J. B. Fletcher, R. Sell, M. J. S. Johnston, R. Durrheim, S. Spottiswoode, and A. Milev. 2009. Broadband records of earthquakes in deep gold mines and a comparison with results from SAFOD, California. *Bulletin of the Seismological Society of America* 99(5):2815-2824.

McGarr, A. 2014. Maximum magnitude earthquakes induced by fluid injection. *Journal of Geophysical Research: Solid Earth* 119(2):1008-1019.

McGuire, R. K. 1995. Probabilistic seismic hazard analysis and design earthquakes: Closing the loop. *Bulletin of the Seismological Society of America* 85(5):1275-1284.

National Earthquake Information Center (NEIC). 2013. U.S. Geological Survey National Earthquake Information Center earthquake catalog. http://earthquake.usgs.gov/earthquakes/search/.

National Research Council (NRC) of the National Academies. 2013. *Induced seismicity potential in energy technologies*. Washington, DC: The National Academies Press.

Notley, K. R. 1983. Rock mechanics analysis of the Springhill mine disaster. *Mining Science and Technology* 1:149-163.

Ogasawara, H., T. Miwa et al. 2002. Ogasawara and the research group for semi-controlled earthquake-generation experiments in South African deep gold mines (1992-2001). In *Seismogenic Process Monitoring*, ed. H. Ogasawara, T. Yanagidani, and M. Ando, 119-150. Tokyo: Balkema.

Oklahoma Corporation Commission (OCC). 2013. The Oklahoma register title 165: Corporation commission chapter 10: Oil and gas conservation. http://www.occeweb.com/rules/Web%20Ready%20Ch10%20FY14%2007-01-13%20searchable.pdf.

Ortlepp, W. D. 1992. Note on fault-slip motion inferred from a study of micro-cataclastic particles from an underground shear rupture. In *Pageoph* 139(¾). Basel, Switzerland: Birkhauser.

Ortlepp, W. D. 2001. Thoughts on the rockburst source mechanism based on observations of the mine-induced shear rupture. *5th International Symposium on Rockbursts and Seismic Activity in Mines, 17-19 September 2001,* S27. Johannesburg, Republic of South Africa.

Ortlepp, W. D., S. Murphy, and G. van Aswegen. 2004. The mechanism of a rockburst – an informative case study. In *Proceedings, 2nd International Seminar on Deep and High Stress Mining*. Johannesburg, Republic of South Africa.

Ortlepp, W. D. 2005. RaSiM comes of age – A review of the contributions to the understanding and control of mine rockbursts. In *Proceedings, 6th International Symposium on Rockbursts and Seismic Activity in Mines, 9-11 March 2005,* ed. Y. Potvin and M. Hudyma. Australia.

Ortlepp, W. D., R. Armstrong, J. A. Ryder, and D. O'Connor. 2005. Fundamental study of micro-fracturing on the slip surface of mine-induced dynamic brittle shear zones. In *Controlling Seismic Risk; Rockbursts and Seismicity in Mines*, ed. Y. Potvin and M. Hudyma, 229-237. Nedlands: Australian Centre for Geomechanics.

Quinn, M. C. L., and O.-D. S. Taylor. 2013. Hazard topography: A multi-hazard approach for dams and levees. In *Proceedings of the 30th annual conference of the Association of State Dam Safety Officials, 8-12 September 2013.* Providence, Rhode Island.

Quinn, M. C. L., and O.-D. S. Taylor. 2014. Hazard topography: A visual approach for identifying critical failure combinations for infrastructure. *Natural Hazards Review, ASCE* 15(2):101-103.

Raleigh, C. B., J. H. Healy, and J. D. Bredehoeft. 1976. An experiment in earthquake control at Rangely, Colorado. *Science* 191(4233):1230–1237.

Richardson, E., and T. H. Jordan. 2002. Seismicity in deep gold mines of South Africa: Implications for tectonic earthquakes. *Bulletin of the Seismological Society of America* 92(5):1766-1782.

Richter, C. F. 1935. An instrumental earthquake scale. *Bulletin of the Seismological Society of America* 25:1-32.

Roen, J. B. 1993. Introductory review – Devonian and Mississippi black shale, eastern North America. In *Petroleum Geology of the Devonian and Mississippi Black Shale of Eastern North America: US Geological Survey Bulletin,* ed. J. B. Roen and R. C. Kepferle, 1909:A1-A8. Reston, VA: USGS.

Scholtz, C. H. 1972. Static fatigue of quartz. *Journal of Geophysical Research.* 77(11):2104-2114.

Scott, D. F., T. J. Williams, and M. J. Friedel. 1997. Investigation of a rockburst site, Sunshine Mine, Kellog, Idaho. In *Proceedings, 4th International Symposium on Rockburst and Seismic Activity in Mines, 11-14 August 1997,* ed. S. J. Gibowicz and S. Lasocki, 311-315. Krakow, Poland.

Seeber, L., J. Armbruster, and W.-Y. Kim. 2004. A fluid-injection-triggered earthquake sequence in Ashtabula, Ohio: Implications for seismogenesis in stable continental regions. *Bulletin of the Seismological Society of America* 94(1):76-87.

Skytruth. 2013. Voluntary disclosure reports submitted by oil and gas drilling operators for hydraulic fracturing operations across the United States, and FracFocus.org. https://s3.amazonaws.com/skytruth_public/2013_FracFocusReport.txt.zip.

Southeastern United States Seismic Network (SUSN). 2013. The Virginia Tech seismological observatory historic/instrumental southeastern U.S. earthquake catalog. http://www.geol.vt.edu/outreach/vtso/anonftp/catalog/.

Spottiswoode, S. M., and A. McGarr. 1975. Source parameters of tremors in a deep-level gold mine. *Bulletin of the Seismological Society of America* 65(1):93-112.

Spotts, P. 2014. Scientists: 'Fracking' should be part of assessing earthquake hazards. http://www.csmonitor.com/Environment/2014/0501/Scientists-Fracking-should-be-part-of-assessing-earthquake-hazards.

Taylor, O.-D. S. 2011. Use of an energy-based liquefaction approach to predict deformation in silts due to pile driving. PhD diss., University of Rhode Island.

Texas Railroad Commission (TRRC). 2014. Hydraulically-fractured gas and injection well locations. http://gis2.rrc.state.tx.us/public/startit.htm.

Turcotte, D. L., E. M. Moores, and J. B. Rundle. 2014. Super fracking. *Physics Today* 67(8):34-39.

USACE. 1970a. *Design and construction of levees*. EM 1110-2-1913. Washington, DC: Department of the Army, Corps of Engineers.

_____. 1970b. *Engineering and design: Stability of earth and rock-fill dams*. EM 1110-2-1902. Washington, DC: Department of the Army, Corps of Engineers.

USACE. 1995. *Earthquake design and evaluation for civil works projects*. ER 1110-2-1806. Washington, DC: Department of the Army, Corps of Engineers.

USACE. 1997. *Risk-based analysis in geotechnical engineering for support of planning studies, 20314-100*. Washington, DC: Department of the Army, Corps of Engineers.

USACE. 2014a. *Safety of dams – Policy and procedures*. ER 1110-2-1156. Washington, DC: Department of the Army, Corps of Engineers.

_____. 2014b. *Selection of design earthquakes and associated ground motions*. Engineering Manual EM 1110-2-6000. Washington, DC: Department of the Army, Corps of Engineers.

_____. 2014c. *Seismic analysis of embankment dams – Including levees*. EM 1110-2-6001. Washington, DC: Department of the Army, Corps of Engineers.

USArray. 2010. *Earthscope transportable array installation plan figure*. http://www.usarray.org/files/images/maps/Install_plan_Dec2010-incl-date-web.jpg.

U.S. Geological Survey (USGS). 2008. U.S. Geological Survey central energy resources team, oil and gas exploration and production in the United States shown as quarter-mile cells. http://geo.gov.ckan.org/harvest/object/74361ccd-3a90-4536-82f4-1d69dc6ee8b5/html.

U.S. Geological Survey (USGS). 2012. National assessment of oil and gas resources team, map of assessed shale gas in the United States. http://pubs.usgs.gov/dds/dds-069/dds-069-z/downloads/.

U.S. Geological Survey (USGS). 2014. Earthquake swarm continues in central Oklahoma. http://www.usgs.gov/newsroom/article.asp?ID=3710#.UvO5kbRrRTs.

USGS. 2013a. Geologic map of U.S. states. http://mrdata.usgs.gov/geology/state/.

_____. 2013b. Quaternary faults in Google Earth. http://earthquake.usgs.gov/hazards/qfaults/google.php.

U.S. Department of Energy. 2009. *Office of fossil energy and national energy technology laboratory, modern shale gas development in the United States: A primer*. Washington, DC: USDOE.

U.S. Energy Information Administration (USEIA). 2011. Geospatial data for basin and play boundaries, data for the U.S. shale plays map. http://www.eia.gov/pub/oil_gas/natural_gas/analysis_publications/maps/tightgasbasinplay.zip.

Utsu, T. 2002. Statistical features of seismicity. In *International handbook of earthquake and engineering seismology*, ed. W. Lee, H. Kanamori, P. Jennings, and C. Kisslinger, 81A. New York: Academic Press.

Wang, Z., and A. Krupnick. 2013. A retrospective review of shale gas development in the United States. *Resources for the Future Discussion Paper*. Washington, DC: Resources for the Future.

Yegian, M. K., E. A. Marciano, and V. G. Ghahraman. 1991. Seismic risk analysis for earth dams. *Journal of Geotechnical Engineering* 117(1):18-34.

Yerkes, R. F., and R. O. Castle. 1976. Seismicity and faulting attributed to fluid extraction. In *Engineering geology,* ed. W.G. Milne, 10(2-4):151-167.

Zou, C. 2013. *Unconventional petroleum geology*. Beijing: Petroleum Industry Press, Elsevier Inc.

REPORT DOCUMENTATION PAGE

Form Approved
OMB No. 0704-0188

Public reporting burden for this collection of information is estimated to average 1 hour per response, including the time for reviewing instructions, searching existing data sources, gathering and maintaining the data needed, and completing and reviewing this collection of information. Send comments regarding this burden estimate or any other aspect of this collection of information, including suggestions for reducing this burden to Department of Defense, Washington Headquarters Services, Directorate for Information Operations and Reports (0704-0188), 1215 Jefferson Davis Highway, Suite 1204, Arlington, VA 22202-4302. Respondents should be aware that notwithstanding any other provision of law, no person shall be subject to any penalty for failing to comply with a collection of information if it does not display a currently valid OMB control number. **PLEASE DO NOT RETURN YOUR FORM TO THE ABOVE ADDRESS.**

1. REPORT DATE (DD-MM-YYYY)	2. REPORT TYPE	3. DATES COVERED *(From - To)*
August 2015	Report 1 of a series	

4. TITLE AND SUBTITLE

Unconventional Hydrocarbon Production Hazard Within The Central United States: Report 1, Overview and Potential Risk To Infrastructure

5a. CONTRACT NUMBER

5b. GRANT NUMBER

5c. PROGRAM ELEMENT NUMBER

6. AUTHOR(S)

Oliver-Denzil S. Taylor, Alanna P. Lester, and Theodore A. Lee III

5d. PROJECT NUMBER

5e. TASK NUMBER

5f. WORK UNIT NUMBER

7. PERFORMING ORGANIZATION NAME(S) AND ADDRESS(ES)

Geotechnical and Structures Laboratory
U.S. Army Engineer Research and Development Center
3909 Halls Ferry Road
Vicksburg, MS 39180-6199

8. PERFORMING ORGANIZATION REPORT NUMBER

ERDC/GSL TR-15-26

9. SPONSORING / MONITORING AGENCY NAME(S) AND ADDRESS(ES)

U.S. Army Corps of Engineers

10. SPONSOR/MONITOR'S ACRONYM(S)

USACE

11. SPONSOR/MONITOR'S REPORT NUMBER(S)

12. DISTRIBUTION / AVAILABILITY STATEMENT

Approved for public release; distribution is unlimited.

13. SUPPLEMENTARY NOTES

14. ABSTRACT

Unconventional hydrocarbon development-induced seismic hazard in historically aseismic regions is more frequent and concentrated than seismicity in established tectonic high-hazard zones. A significant increase in seismicity within historically aseismic regions and in close proximity to federal infrastructure has been observed within Arkansas, Kentucky, Missouri, Oklahoma, Tennessee, Texas, and Virginia. Seismological events **M**2.0 and greater, spanning 02/08/1950 until 10/20/2013, were analyzed to identify and assess the hazard potential. Geospatial and temporal observations correlate the seismic increase to the rise of unconventional hydrocarbon development, which has become more analogous with deep ore mining in terms of energy release. Thus, unconventional hydrocarbon is subjected to the same causality phenomena and associative hazards with significant implications towards quantifying the risk to infrastructure health and longevity. Furthermore, the current standard of practice for risk assessment is not applicable for this highly variable, induced hazard. Additionally, this research investigated the cumulative seismic potential, based on injected fluid volume, of co-located hydraulic fracturing wells wherein the seismic potential of such wells are equivalent to the seismic potential of conventional wastewater injection wells. This cumulative seismic potential of multiple hydraulic fracturing wells could explain the seismicity within regions of Arkansas, Oklahoma, and Texas, wherein no other regional geo-engineering activity has been reported. Additionally, this study presents a power-law relation, useful for all injected fluid activities irrespective of the injection purpose, and applies the cumulative potential to the largest known UHP hydraulic fracturing volumes an event up to M_w5.5 can reasonably expect with a maximum potential of M_w6.5

15. SUBJECT TERMS		
Unconventional Hydrocarbon Development	Induced Seismicity	Observation data
	Earthquakes	Risk
	Hydraulic Fracturing	Hazard Identification

16. SECURITY CLASSIFICATION OF:			17. LIMITATION OF ABSTRACT	18. NUMBER OF PAGES	19a. NAME OF RESPONSIBLE PERSON
a. REPORT	b. ABSTRACT	c. THIS PAGE			19b. TELEPHONE NUMBER *(include area code)*
UNCLASSIFIED	UNCLASSIFIED	UNCLASSSIFIED		62	